

To the Editor

We thank the Editor for her efficient handling of our manuscript at Biogeosciences. We have now addressed all the comments posted by the three Reviewers. Additional data and major changes in the revised manuscript include:

- Pore water SO_4^{2-} , Ca^{2+} , Mg^{2+} and Mn^{2+} concentrations (Figure 2a)
- Geochemical modeling of pore water major ions (Table 1)
- Downcore profiles for both highly reactive and total iron in bulk sediment (Figure 2a)
- Corrections of the methods (pore water PO_4^{3-} , Fe^{2+} , Fe^{3+})
- Rewriting of the discussion on Fe isotopes that now includes a description of source-to-sink processes and their influence on Lake Towuti's Fe mineralogy. We compare the dataset of the present ferruginous analogue (i.e. Fe minerals, concentrations of pore water solutes) to the one interpreted from the ancient rock record and provide clues on how to discriminate past environmental conditions from early diagenetic processes.

Please find hereafter our point-by-point answers to each comment and criticism brought by the three Reviewers. The corresponding changes in the revised manuscript presently submitted are highlighted in red font. We would like to assure the Editor that we are eager to meet the criteria for publication in Biogeosciences and remain at your disposition for further information. We are looking forward to the outcome of your deliberations. On behalf of all the authors,

Yours sincerely

Aurèle Vuillemin
(first/corresponding author)

Reviewer 1

We thank the Reviewer for his/her careful review of our manuscript, which highly helped us improving the new version of the manuscript presently submitted. We have addressed all of the Reviewer's concerns with new additional data, namely:

- Pore water SO_4^{2-} , Ca^{2+} , Mg^{2+} and Mn^{2+} concentrations were added to Figure 2a and are discussed in the revised manuscript
- Based on geochemical modeling of pore water major ions, we calculated saturation indices for specific minerals. The revised manuscript contains a new table listing saturation indices for diagenetic minerals relevant of the present system (e.g. vivianite, siderite, calcite).
- The description of the methods and results (SO_4^{2-} , PO_4^{3-} , Fe^{2+} , Mn^{2+} , Ca^{2+} , Mg^{2+}) has been carefully reviewed and corrected.

We did our best to fulfill all the remarks and suggestions brought by the Reviewer. Each comment has been addressed in separate answers, and all the corresponding changes are highlighted in red in the text. Please, find here after our point by point answers to Reviewer 1.

Yours sincerely,

Aurèle Vuillemin

Specific comments

Section 2.4

- line 27: Phosphate was measured by ion chromatography. This method has the disadvantage of having a rather poor detection limit. The authors announce a limit of quantification of 14.3 μM , which is insufficient here. Commonly used colorimetric methods give at least 20x better detection. The main problem here is that all the concentrations presented in pore water are between 0 and 1 μM , well below the limit of quantification. Figure 2 shows a PO_4 profile with variations between 0 and 1 μM . There is therefore a problem with these PO_4 data, either in the description of the method or in the results; this must be seriously corrected.

Answer 1: Thank you for detecting this serious mistake from our side. By inadvertence, we reported the method used for major ion quantification. We indeed measured phosphate concentrations using spectrophotometry. We corrected the corresponding method part as follows:

"Concentrations of PO_4^{3-} in pore water were measured by spectrophotometry. We aliquoted 0.5 mL pore water to 1.5 mL disposable cuvettes (Brand GmbH, Germany) and added 80 μL color reagent consisting of ammonium molybdate containing ascorbic acid and antimony (Murphy and Riley, 1962). Absorbance was measured at 882 nm with a DR 3900 spectrophotometer (Hach, Düsseldorf, Germany). Detection limit of the method is 0.05 μM ."

Additional reference:

- Murphy, J., and Riley, J. P.: A modified single solution method for the determination of phosphate in natural waters
Anal. Chim. Acta, 27, 31-36, 1962.

- line 29: pH is measured in the supernatant after homogenization of 2 mL sediment in 2 mL deionized water. I have never seen that the pH of pore water can be measured in this way. Is there a reference? The pH is measured here in pore water diluted with deionized water. This cannot give the in-situ pH value. In addition, the authors solve the carbonate system with this questionable pH measurement. Why did the authors not measure the pH in the water used to measure alkalinity?

Answer 2: What we presently applied is a method commonly used to measure pH in soil samples. We followed the published method no. 9045B from Black (1973) and calibrated our results based on the Standard Reference Material Catalog (Seward, 1986). This information has been added to the text.

"We homogenized 2 mL of sediment in 2 mL of deionized water and measured the supernatant after 2 min, which is the method commonly used to measure pH in organic-rich soil samples. We followed the published method no. 9045B from Black (1973) and calibrated our results based on the Standard Reference Material Catalog (Seward, 1986)."

Additional references:

- Black, C. A. (Ed.): Methods of Soil Analysis: Test Methods for Evaluating Solid Waste, Physical/Chemical Methods, 9045B Soil and Waste pH, American Society of Agronomy, Madison, USA, 1973.
- Seward, R. W. (Ed.): NBS Standard Reference Material Catalog NBS, Special Publication 260, National Bureau of Standards, Gaithersburg, USA, 1986-1987.

Section 3.4

- line 25: "Given that vivianite is a Fe^{2+} -bearing mineral phase, the isotopically light $\delta^{56}\text{Fe}$ values we measured in vivianites from Lake Towuti are consistent with the direction of fractionation occurring during Fe^{3+} reduction."

This interpretation is based on the principle that $\text{Fe}(\text{II})$ is the result of the reduction of $\text{Fe}(\text{III})$. But there is no evidence of that. The interpretation given here is indeed the one that would be given for "classical" sediments. But here, the context is very particular and it cannot be excluded that the Fe^{2+} that produced the vivianite does not come from the dissolution of an initial $\text{Fe}(\text{II})$ phase. This point should be discussed.

Answer 3: We modified this sentence in part 3.4 with the following statement:

"...are consistent with the direction of fractionation occurring during Fe^{3+} reduction. However, dissolution of precursory ferrous phases could also be the source of the Fe^{2+} incorporated in vivianite crystals."

We rewrote most of section 4.3 in the discussion in order to address Towuti's Fe mineralogy in terms of source to sink processes. We discuss the dissolution of initial and transient ferric/ferrous phases, the neoformation of minerals in the sediment and the related redistribution of Fe isotopes during reductive

diagenesis. We use new pore water data (i.e. Mn^{2+} , Ca^{2+} , Mg^{2+} and SO_4^{2-} concentrations) and modeled saturation indices for vivianite and siderite to support our interpretations (see answer no. 13).

Section 4.1

- **p.11, first paragraph:** “The ferrous Fe and P released from these reactions may produce vivianite, and/or be consumed through reactions with other dissolved elements, such as S.”

This first paragraph is not precise enough and is based on too many insinuations. Be more specific.

Answer 5: We replaced this sentence by the following one:

“In aquatic systems and surface sediments, Fe chemistry influences the distribution of dissolved sulfide, the solubility of trace metals, and bioavailability of phosphorus and thereby controls their rates of burial (Severmann et al., 2006)...”

Additional reference:

- Severmann, S., Johnson, C. M., Beard, B. L., and McManus, J.: The effect of early diagenesis on the Fe isotope compositions of porewaters and authigenic minerals in continental margin sediments, *Geochim. Cosmochim. Ac.*, 70, 2006-2022, <https://doi.org/10.1016/j.gca.2006.01.007>, 2006.

- **line 8 and 13:** HS^- and H_2S .

Answer 6: H_2S modified to HS^- consistently throughout the text.

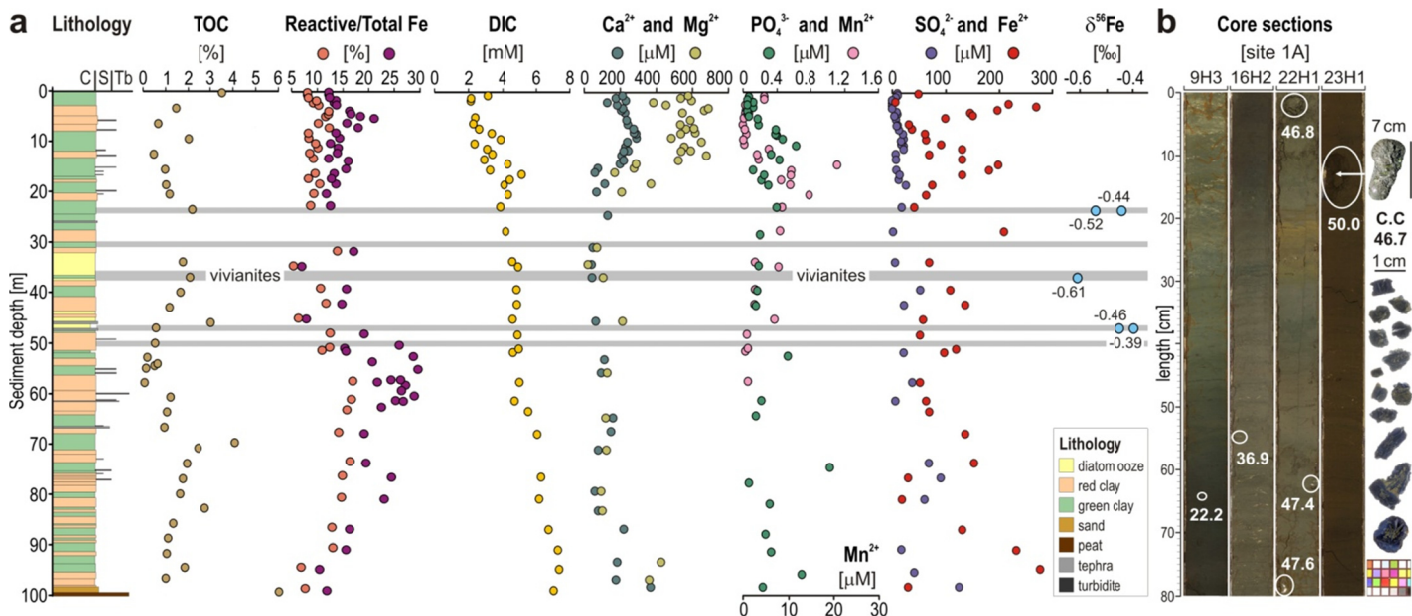
- **line 16** “Because rates of sulfide production are so low compared to the Fe delivery flux” and “in sediments such as Lake Towuti’s, siderite is an expected mineral phase” What are the quantitative elements to assert this?

Answer 7: We implemented pore water SO_4^{2-} concentrations to Figure 2a (here under). With the exception of four data points (i.e. 85, 81, 107, 121 μM), SO_4^{2-} concentrations are systematically below 50 μM and are on average 27 μM over the whole profile, which confirms quantitatively that production of HS^- in pore water is limited.

We also modeled mineral saturation indices based on the complete pore water dataset using the PHREEQC v.3 software, inclusive of all major cations (Na^+ , NH_4^+ , K^+ , Mg^{2+} , Ca^{2+} , Si^{4+} , Fe^{2+} , DIC), anions (Cl^- , SO_4^{2-} , NO_3^- , PO_4^{3-}), alkalinity, pH and borehole temperatures. These results show that pore water is oversaturated with respect to siderite (>0) in the entire sediment column, whereas vivianite remains close to, but slightly below saturation (-0.04). We report these modeled indices in a new table (Table 1, here under) and implemented the manuscript accordingly.

Additional reference:

- Parkhurst, D. L., and Appelo, C. A. J. (Eds.): Description of input and examples for PHREEQC version 3: a computer program for speciation, batch-reaction, one-dimensional transport, and inverse geochemical calculations, book 6, chapter A43: U.S. Geological Survey Techniques and Methods, Denver, USA, 2013.



Revised Figure 2

5 m depth	Saturation	10 m depth	Saturation
talc	1.43	siderite	1.00
siderite	1.29	quartz	0.71
quartz	0.71	vivianite	-0.04
vivianite	-0.45	talc	-0.31
calcite	-0.68	calcite	-0.83
dolomite	-0.77	aragonite	-0.97
aragonite	-0.82	dolomite	-1.27

Table 1

- **line 27:** “Because of the high concentrations of Fe oxides in Lake Towuti’s sediment (20 wt %), it is very unlikely that much P could escape to the bottom water.”

This is another unjustified statement. If the ferric phases have their PO₄ adsorption sites saturated, PO₄ can migrate.

Answer 8: We rephrased the second part of this sentence as follows:

“Concentrations of Fe oxides in Lake Towuti’s sediment are high (~ 20 wt %), and iron oxides such as goethite persist in the modern sediment even under full anoxia at the water-sediment interface and below (Sheppard et al., 2019). If PO₄³⁻ could diffuse out of the sediment,…”

- **line 30:** “In the deep sediments, pore water PO_4^{3-} concentrations are constantly low in the interval where vivianite crystals are observed (Fig. 2a), suggesting that vivianites acted as a main P sink during diagenesis”.

PO_4 concentrations are not quantified, given the method used. Are there not the elements to calculate the theoretical concentration of PO_4 that would be at thermodynamic equilibrium with vivianite? Such a calculation could strengthen the assertions.

Answer 9: As mentioned in answer no. 1, we corrected the description of the method. Since PO_4^{3-} concentrations were measured via spectrophotometry, our values can be considered reliable and quantitatively sound. As explained in answer no. 7, we also modeled mineral saturation indices based on the complete pore water dataset, which provide theoretical values on pore water saturation with respect to both siderite and vivianite. This new data is available as Table 1.

- **p. 12, line 18:** “they are...rather subject to variety of processes that are variable down core.”

The conclusion of this paragraph reflects its vague and speculative nature. The processes mentioned should be better described. Methane production suddenly appears without any other explanation. It would be better to specify the presentation.

Answer 10: We deleted this part of the sentence. We rephrased the sentences discussing methanogenic conditions and the role of CO_2 reduction by methanogenic archaea in controlling pore water activity of dissolved CO_3^{2-} ions. We also implemented Figure 2a with pore water Ca^{2+} , Mg^{2+} and Mn^{2+} concentrations and discuss their role in controlling PO_4^{3-} solubility and reactivity toward Fe^{2+} . The text (p. 12-13, lines 30-9) was modified as follows:

“...In contrast, Fe^{3+} concentrations in pore water are already depleted along the upper meter of sediment, whereas concentrations of DIC, which is produced during OM degradation, gradually increase with depth (Fig. 2a), suggesting that OM remineralization in shallow sediment is mainly driven by fermentation and methanogenesis rather than microbial Fe reduction (Vuillemin et al., 2018). In the vivianite-bearing intervals, DIC concentrations remain rather constant (4 mM). An explanation for this is that, once pore water Fe^{3+} and SO_4^{2-} concentrations are depleted as a result of microbial reduction within the first meter, OM remineralization mostly occurs by CO_2 reduction and methanogenesis (Friese et al., 2018). The onset of autotrophic methanogenesis is expected to reduce DIC activity in pore water and to draw down PO_4^{3-} cycling by microbes. Moreover, Ca^{2+} and Mg^{2+} concentrations in pore water, which are predicted to control the solubility of PO_4^{3-} in ferruginous systems (Jones et al., 2015), drop around these depths as divalent cations can precipitate during siderite formation (Vuillemin et al., 2019a), suggesting that PO_4^{3-} can then outcompete CO_3^{2-} for available Fe^{2+} and thereby saturate pore water with respect to vivianite (Table 1). Vivianite formation is indeed reported to occur under methanogenic conditions, often initiating below the sulfate-methane transition zone (Reed et al., 2011; Dijkstra et al., 2016), presently located within the upper meter of sediment (Vuillemin et al., 2018). Inclusions of millerite and siderite within vivianite crystals (Fig. 4) provide additional lines of evidence for microbial processes of pore water Fe^{3+} and SO_4^{2-} reduction with DIC production prior to vivianite formation. The saturation indices modeled for vivianite (Table 1) and downcore profiles of Mn^{2+} and PO_4^{3-} concentrations allow to infer a depth in the sediment at which pore waters initially reached saturation with respect to vivianite (ca. 20 m depth). Such relationship between dissolved Mn^{2+} and

PO_4^{3-} is also consistent with EDX punctual analyses of vivianite crystals that show Mn^{2+} incorporation at an early stage (Fig. 3b, Supplementary Fig. S4)....”

Additional references:

- Friese, A., Kallmeyer, J., Glombitza, C., Vuillemin, A., Simister, R., Nomosatryo, S., Bauer, K., Heuer, V. B., Henny, C., Crowe, S. A., Ariztegui, D., Bijaksana, S., Vogel, H., Melles, M., Russell, J. M., and Wagner, D.: Methanogenesis predominates organic matter remineralization in a ferruginous, non-sulfidic sedimentary environment, EGU General Assembly Conference Abstracts , 20, 7446, 2018.
- Jones, C., Nomosatryo, S., Crowe, S. A., Bjerrum, C. J., and Canfield, D. E.: Iron oxides, divalent cations, silica, and the early earth phosphorus crisis, Geology, 43, 135-138, <http://doi.org/10.1130/G36044.1>, 2015.

- **line 29:** “The presence of diatomaceous oozes, with vivianites below and above these sediments, indicates that P concentrations in the water column were much higher during this time interval compared to present-day levels”

The authors suggest here that the fossilization of more diatoms suggests that primary production was higher at the time of these deposits and that the increase in primary production was due to an increase in phosphate inputs. If this is the case, it should be detailed as such. But I am not sure that this is necessarily the case, because the exact opposite can be interpreted. Indeed, one could also imagine that an increase in eutrophication due to PO_4 input would favor cyanobacteria rather than diatoms, as observed in many lakes. Thus, more diatoms could indicate less PO_4 . This should be discussed. In addition, the preservation of diatoms may also come from conditions more favorable to their fossilization than other periods.

Answer 11: We modified this sentence and added another one to address primary productivity by diatoms and cyanobacteria under increased P concentrations and their relative preservation in the sediment. These two sentences are as follows:

“...The substantial fossilization of diatoms, with vivianites below and above these sediments, could reflect higher P concentrations in the water column during this time interval compared to present-day levels...”

“...As P concentrations tend to affect algal phytoplankton productivity as a whole (Zhang and Prepas, 1996; Van der Grinten et al., 2004), high Si concentrations in the lake represent an additional factor promoting the preservation of diatoms over cyanobacteria during sinking and burial....”

Additional references:

- Van der Grinten, E., Janssen, M., Simis, S. G. H., Barranguet, C., and Admiraal, W.: Phosphate regime structures species composition in cultured phototrophic biofilms, Freshwater Biol., 49, 369-381, <https://doi.org/10.1111/j.1365-2427.01189.x>, 2004.
- Zhang, Y., and Prepas, E. E.: Regulation of the dominance of planktonic diatoms and cyanobacteria in four eutrophic hardwater lakes by nutrients, water column stability, and temperature, Can. J. Fish. Aquat. Sci., 53, 621-633, <https://doi.org/10.1139/f95-205>, 1996.

Section 4.3

- **line 12:** “Dissimilatory microbial reduction of iron releases Fe^{2+} in pore water that is up to 2 ‰ lighter than the original substrates ” the fractioning will depend on the rate of reduction.

Answer 12: Agreed. We modified the first part of this paragraph as follows:

“Previous Fe isotope studies of lakes identified either partial oxidation of Fe^{2+} in the water column or microbial iron reduction below the sediment-water interface as the main drivers for Fe pathways and isotope fractionation (Teutsch et al., 2009; Song et al., 2011; Liu et al., 2015). Depending on rates of Fe reduction and dissolution (Brantley et al., 2001), dissimilatory microbial reduction of iron releases Fe^{2+} that is up to 2 ‰ lighter than the original substrates (Crosby et al., 2007; Tangalos et al., 2010), therefore iron isotopes are commonly used to trace redox processes related to microbial activity in aquatic sediments (Percak-Dennett et al., 2013; Busigny et al., 2014)....”

- **line 21:** $\delta^{56}\text{Fe}$ values measured on vivianite are compared to “expected” values for iron oxides. From this point on, all the following in this paragraph is speculative and not supported by data.

Answer 13: As mentioned in answer no. 3, the second paragraph of section 4.3 was entirely rewritten to present Towuti’s Fe mineralogy in terms of source to sink processes. We address the dissolution of initial and transient ferric/ferrous phases, the neoformation of minerals in the sediment and the related redistribution of Fe isotopes during reductive diagenesis. We further refer to previous publications on Towuti’s Fe mineralogy (Tamuntuan et al., 2015; Sheppard et al., 2019), and use new pore water data (i.e. Ca^{2+} , Mg^{2+} and SO_4^{2-} concentrations) and modeled saturation indices to support our interpretations. The second part of section 4.3 was modified as follows:

“Compared to the global bulk igneous rock reservoir ($\delta^{56}\text{Fe} = +0.1 \pm 0.1 \text{ ‰}$) and ultramafic rocks (Dauphas et al. 2017) such as those present in Lake Towuti’s catchment, the $\delta^{56}\text{Fe}$ measured on whole vivianite crystals (-0.61 to -0.39 ‰) reveals incorporation of isotopically fractionated light Fe^{2+} (Fig. 2a), even though traces of detrital iron-bearing minerals and secondary oxides are present within vivianite crystals (Figs 4 and 5). Towuti’s Fe mineralogy from source to sink reflects complex cycling of Fe as iron minerals derived from catchment soils (e.g. goethite, hematite, magnetite) tend to transform into nanocrystalline Fe phases during reductive dissolution in the lake water column and sediment (Tamuntuan et al., 2015; Sheppard et al., 2019). Ferric/ferrous phases precipitating in equilibrium at the oxycline or during mixing events could be abiotically fractionated to 1-2 ‰ heavier/lighter isotope values than the remaining aqueous Fe^{2+} (Bullen et al., 2001; Skulan et al., 2002; Beard et al., 2010; Wu et al., 2011). After deposition, partitioning of the light Fe isotopes mainly transits through release to pore water (Henkel et al., 2016) implying a succession of mineral transformation and dissolution with internal diagenetic Fe redistribution during burial (Severmann et al., 2006; Scholz et al., 2014). For instance, mixed-valence iron oxides (e.g. green rust), which are authigenic phases that form initially under ferruginous conditions (Zegeye et al., 2012; Vuillemin et al., 2019a) are highly sorbent for pore water HCO_3^- and HPO_4^{2-} and can thereby transform into either siderite or vivianite as the sediment ages (Hansen and Poulsen, 1999; Bocher et al., 2004; Refait et al., 2007; Halevy et al., 2017). Because vivianite formation initiates in the sediment, we infer that vivianite crystals acted as additional traps for the reduced Fe^{2+} released to pore water and that their light $\delta^{56}\text{Fe}$ values are consistent with kinetic

fractionation related to microbial Fe reduction during early diagenesis, or eventually inherited from post-depositional dissolution of transient ferrous phases. In the latter case, pre-depositional processes of abiotic Fe fractionation related to stratified conditions will require further investigations.”

Additional references:

- Bocher, F., Géhin, A., Ruby, C., Ghanbaja, J., Abdelmoula, M., and Génin, J.-M. R.: Coprecipitation of Fe(II–III) hydroxycarbonate green rust stabilized by phosphate adsorption, *Solid State Science*, 6, 117–124, <https://doi.org/10.1016/j.solidstatesciences.2003.10.004>, 2004.
- Brantley, S. L., Liermann, L., and Bullen, T. D.: Fractionation of Fe isotopes by soil microbes and organic acids, *Geology*, 29, 535–538, [https://doi.org/10.1130/0091-7613\(2001\)029<0535:FOFIBS>2.0.CO;2](https://doi.org/10.1130/0091-7613(2001)029<0535:FOFIBS>2.0.CO;2), 2001.
- Halevy, I., Alesker, M., Schuster, E. M., Popovitz-Biro, R., and Feldman, Y.: A key role for green rust in the Precambrian oceans and the genesis of iron formations, *Nat. Geosci.*, 10, 135–139, <https://doi.org/10.1038/ngeo2878>, 2017.
- Hansen, H. C. B., and Poulsen, I. F.: Interaction of synthetic sulphate "green rust" with phosphate and the crystallization of vivianite, *Clay. Clay Miner.*, 47, 312–318, doi: 10.1346/CCMN.1999.0470307, 1999.
- Henkel, S., Kasten, S., Poulton, S. W., and Staubwasser, M.: Determination of the stable iron isotopic composition of sequentially leached iron phases in marine sediments. *Chem. Geol.* 421, 93–102, <https://doi.org/10.1016/j.chemgeo.2015.12.003>, 2015.
- Refait, P., Reffass, M., Landoulsi, J., Sabot, R., and Jeannin, M.: Role of phosphate species during the formation and transformation of the Fe(II–III) hydroxycarbonate green rust, *Colloid. Surface A*, 299, 29–37, doi: 10.1016/j.colsurfa.2006.11.013, 2007.
- Scholz, F., Severmann, S., McManus, J., Noffke, A., Lomnitz, U., and Hensen, C.: On the isotope composition of reactive iron in marine sediments: Redox shuttle versus early diagenesis. *Chem. Geol.*, 389, 48–59, <https://doi.org/10.1016/j.chemgeo.2014.09.009>, 2014.
- Severmann, S., Johnson, C. M., Beard, B. L., and McManus, J.: The effect of early diagenesis on the Fe isotope compositions of porewaters and authigenic minerals in continental margin sediments, *Geochim. Cosmochim. Ac.*, 70, 2006–2022, <https://doi.org/10.1016/j.gca.2006.01.007>, 2006.

- Last sentence of the conclusion: “Although crystallization time was not constrained, supply of pore water PO_4^{3-} and Fe^{2+} during diagenesis maintained saturation with respect to vivianite and supported the continuous growth of crystals with depth.”

Here again, this statement is not validated by calculations. The degree of water saturation with respect to vivianite has not been calculated.

Answer 14: We deleted this sentence. As mentioned in answer no. 7, the revised manuscript now includes a new table of modeled saturation indices (Table 1) showing that pore water reaches conditions that are very close to saturation with respect to vivianite with depth. If pore water PO_4^{3-} was indeed incorporated in vivianite crystals during burial, this PO_4^{3-} cannot be accounted for in the pore water modeling. One can thus only infer a timeframe during which geochemical conditions in pore water were saturated with respect to vivianite. In this context, the downcore profiles for pore water Mn^{2+} and PO_4^{3-} concentrations allow to infer the depth at which pore waters reach initial saturation with respect to vivianite (ca. 20 m depth).

Technical corrections

- **Section 2.1, line 10:** Describe in more detail the chronology of the operations, i.e. date of drilling, extraction of pore water.... the minerals were extracted after more than 6 months of storage. Please specify it.

Answer 15: For detailed information on field sampling and core processing, the readership can refer to (Russell et al., 2016; Friese et al., 2017). Following the Reviewer's suggestion, we implemented part 2.1 as follows:

"The TDP coring operations were carried out from May to July 2015 using the International Continental Scientific Drilling Program (ICDP) Deep Lakes Drilling System (Russell et al., 2016). Hole TDP-TOW15-1A (156 m water depth; hereafter TDP-1A) was drilled in May 2015 with a fluid contamination tracer used to aid geomicrobiological sampling (Friese et al., 2017). Samples were collected from cores from TDP-1A immediately upon recovery and over 450 samples were subsequently processed in the field for analyses of pore-water chemistry, cell counting and microbial fingerprinting, and organic geochemistry. Core catchers from TD-1A were packed into gas-tight aluminum foil bags flushed with nitrogen gas and heat-sealed to keep them under anoxic conditions until mineral extraction. Pore water was extracted on site from 5-cm-long whole round cores (6.6 cm diameter) that were cut from the core sections, immediately capped and transferred to an anaerobic chamber flushed with nitrogen to avoid oxidation during sample handling (Friese et al., 2017). In January 2016, the unsampled remainders of the cores from TDP-1A were split and scanned at the Limnological Research Center, Lacustrine Core Facility (LacCore), University of Minnesota, described macroscopically and microscopically to determine their stratigraphy and composition (Russell et al., 2016) and then subsampled. Minerals from core catcher sediments were extracted after 3 month of storage, and macroscopically visible vivianite crystals were hand-picked from split TDP-1A cores after 8 months of storage. Except as otherwise noted, all our samples and measurements come primarily from hole TDP-1A."

- **Section 2.2, line 24:** The carbonate removal technique to measure the total organic carbon goes through a washing and centrifugation phase. Doesn't this step cause the loss of organic matter less dense than water?

Answer 16: This is the standard procedure applied for TOC and bulk organic matter using HCl (5%) on freeze-dried samples. We tested this method on pure siderite to ensure that this carbonate phase dissolves in the same way as calcite. Such sample processing is routine analysis at the Forschungszentrum Jülich.

- **Section 2.4, line 17:** Dissolved Fe is measured using Ferrozine. Authors have used the method described by Viollier et al., 2000. This study recommends using ascorbic acid to transform all dissolved iron (FeII + FeIII) into FeII. Was ascorbic acid used here?

Answer 17: In Viollier et al., (2000), the authors mention the addition of hydroxylamine hydrochloride as the reducing agent used to measure pore water Fe^{3+} , and not ascorbic acid as stated by the reviewer (which is included in the measurement of PO_4^{3-} concentrations). Fe^{3+} concentrations can be calculated as the difference between total Fe and Fe^{2+} . We did process the samples using hydroxylamine hydrochloride and therefore we corrected the method description part accordingly. However, total Fe concentrations measured in pore water were identical to those of Fe^{2+} , and thus Fe^{3+} is absent in pore water. We also referenced the initial protocol from Stookey (1970). The method part was revised as follows:

“Dissolved ferrous and ferric iron concentrations were measured in the field via spectrophotometry (Stookey, 1970). Directly after pore water retrieval, we aliquoted 1 mL of pore water sample to 1.6 mL Rotilabo single-use cells (Carl Roth, Karlsruhe, Germany) and stabilized dissolved Fe^{2+} by adding 100 μL of Ferrozine Iron Reagent (Sigma-Aldrich Chemie Munich, Germany). Absorbance of the colored solution was measured at 562 nm with a DR 3900 spectrophotometer (Hach, Düsseldorf, Germany). To determine pore water total Fe concentrations, 150 μL of hydroxylamine hydrochloride were added to 800 μL of the previous mixture, left to react 10 min to reduce all dissolved Fe^{3+} , stabilized by adding 50 μL ammonium acetate and absorbance of the solution measured a second time (Viollier et al., 2000). Pore water total Fe concentrations were found to be the same as Fe^{2+} concentrations, and thus Fe^{3+} is absent in pore water. Detection limit of the method is 0.25 μM .”

Additional reference:

- Stookey, L. L.: Ferrozine - A new spectrophotometric reagent for iron, *Anal. Chem.*, 42, 779-781, <https://doi.org/10.1021/ac60289a016>, 1970.

Reviewer 2

We thank the Reviewer for his/her careful review of our manuscript, which helped us improving the new version of the manuscript presently submitted. We have addressed all of the Reviewer's concerns with additional data, namely:

- Pore water SO_4^{2-} , Mn^{2+} , Ca^{2+} and Mg^{2+} concentrations were added to Figure 2a and are discussed in the revised manuscript.
- Downcore profiles for both highly reactive and total iron in bulk sediment are provided in Figure 2a.
- Based on geochemical modeling of pore water major ions, we calculated saturation indices for specific minerals (e.g. vivianite, siderite). These indices are listed in a new table (Table 1) now included in the revised manuscript.

We did our best to fulfill all the remarks and suggestions brought by the Reviewer. Each comment has been addressed in separate answers, and all the corresponding changes are highlighted in red in the text. Please, find here after our point by point answers to Reviewer 2.

Yours sincerely,

Aurèle Vuillemin

Major comments

- **Comment 1:** The authors should clarify and emphasize their findings. For example, the authors should present an important finding regarding vivianite formation already in the title. The same applies to the abstract and later on, and what is novel regarding the formation of vivianite should be emphasized here in comparison to previous publications (e.g. Slomp, Paytan, Marz, Kasten).

Answer 1: We changed the title to "Microbially mediated formation of vivianite during early diagenesis in ferruginous sediments, Lake Towuti, Indonesia."

We implemented the abstract with the following sentences to emphasize, as expressly demanded, the novelty and implications of our findings:

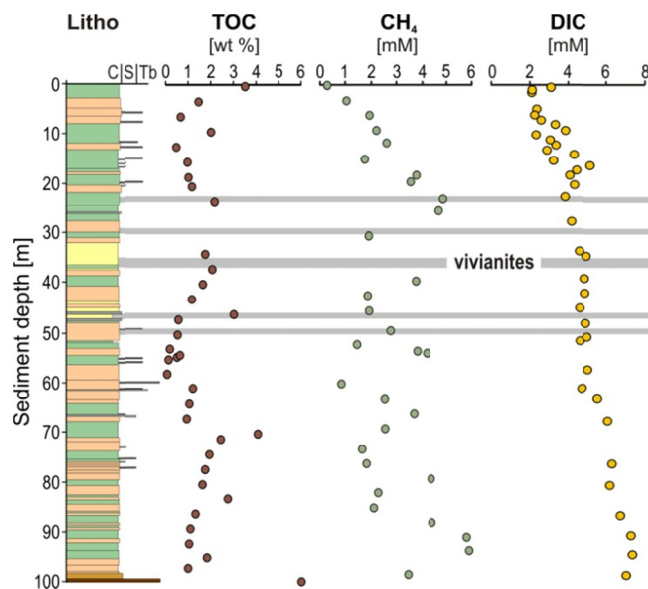
"...Together with pore water profiles, these suggest that the precipitation of millerite, siderite, and vivianite in soft ferruginous sediments stems from the gradual microbial reduction of pore water electron acceptors. Based on solute concentrations and modeled mineral saturation indices, we inferred vivianite formation to initiate around 20 m depth in the sediment as the likely result of the decrease in microbial activity and associated P recycling in pore water. Negative $\delta^{56}\text{Fe}$ values of vivianite indicated incorporation of kinetically fractionated light Fe^{2+} into the crystals, likely derived from active reduction and dissolution of ferric oxides and transient ferrous phases during early diagenesis. The size and growth history of the nodules indicate that, after formation, continued growth of vivianite crystals constitutes a sink for P during burial, resulting in long-term P sequestration in ferruginous sediment."

- **Comment 2:** It is hard to judge the vivianite formation in response to paleoconditions, because: there is no quantitative investigation of the amounts of vivianite; there is a lack of context on pore water redox conditions in the vivianite-bearing layers (e.g. SMTZ redox sensitive elements other than iron). Where are the other pore water profiles (at least Mn^{2+} , SO_4^{2-} , methane)?

Answer 2: We provide additional pore water data, namely downcore profiles for SO_4^{2-} , Ca^{2+} , Mg^{2+} , and Mn^{2+} concentrations. The downcore profile for Mn^{2+} concentrations (revised Figure 2a) covaries with PO_4^{3-} and correlates the increased Mn content measured via EDX on early stage vivianite crystals. This, in addition to the saturation indices modeled for siderite and vivianite (Table 1), allows us to infer the depth at which pore waters reach initial saturation with respect to vivianite (see answer no. 3).

We emphasize in the manuscript the depth inferred for the SMTZ, which, due very low SO_4^{2-} concentrations, is located within the upper 50 cm of sediments. This was already addressed in a previous publication based on gravity cores (VUILLEMIN et al., 2018, Environ. Microbiol. 20).

Concerning methane concentrations, because a manuscript addressing methane production is presently under review, we refrain from providing this data. Since there is no preprint for this manuscript, we only cite an abstract related to the manuscript (Friese et al., 2018; EGU abstract). To answer the Reviewer's demand, we provide at his/her discretion an insight into methane concentrations here under, which confirms that the SMTZ is found in very shallow sediments and that methane concentrations constantly increase with sediment depth. The trend for methane is similar to the one of DIC.



Because vivianites are only observed from 20 to 50 m depth intercalated with diatom oozes, we further addressed paleoproductivity and changes in the sedimentary regime. Still, we consider that we provide clear and sufficient evidence for the microbially mediated formation of vivianite during early diagenesis (see answer no. 9). We would also like to bring to the attention of the Reviewer that analyses for paleoenvironmental reconstructions are ongoing work and that a first manuscript detailing the lithostratigraphy and sedimentological processes is close to being submitted. The age model, which is the

most critical aspect in reconstructing past climate, is still under preparation. In the meanwhile, one has to accept some inferences and avoid speculations.

Additional references:

- Friese, A., Kallmeyer, J., Glombitza, C., Vuillemin, A., Simister, R., Nomosatryo, S., Bauer, K., Heuer, V. B., Henny, C., Crowe, S. A., Ariztegui, D., Bijaksana, S., Vogel, H., Melles, M., Russell, J. M., and Wagner, D.: Methanogenesis predominates organic matter remineralization in a ferruginous, non-sulfidic sedimentary environment, EGU General Assembly Conference Abstracts , 20, 7446, 2018.

- **Comment 3:** The paleointerpretation is confusing (page 12). When was the vivianite precipitated in the 20-50 m interval: Thousands years ago at the bottom of the lake or now due to current diagenetic processes? More data and discussion (e.g. diffusion modeling) are needed to support the first or second option. Otherwise, it is hard to suggest environmental interpretations without putting the current diagenetic processes into context or quantifying inferred past processes.

Answer 3: We now provide saturation indices modeled for specific minerals (e.g. vivianite, siderite) in a new table (Table 1, here under). These results show that siderite is the main mineral to reach saturation in the pore water at relatively shallow sediment depths (5 m), and that the saturation index modeled for vivianite increases with depth, but remains slightly below saturation. This, in addition to pore water concentrations (i.e. Mn^{2+} , Ca^{2+} , Mg^{2+}), allows to infer the depth at which pore waters are initially saturated with respect to vivianite, which is about 15 m depth. We consider that the downcore profile for pore water Mn^{2+} and PO_4^{3-} in parallel confirms this and correlate the increased Mn content measured on vivianite crystals via EDX and its incorporation at an early stage of growth.

5 m depth	Saturation	10 m depth	Saturation
talc	1.43	siderite	1.00
siderite	1.29	quartz	0.71
quartz	0.71	vivianite	-0.04
vivianite	-0.45	talc	-0.31
calcite	-0.68	calcite	-0.83
dolomite	-0.77	aragonite	-0.97
aragonite	-0.82	dolomite	-1.27

Table 1

Specific comments

Abstract

The first sentence is not relevant as it refers to ferric iron and phosphate adsorption and not to vivianite. Rewrite a general sentence that states that ferruginous lakes are important to the phosphorous cycle because of X, Y, etc.

Answer 4: We rephrased the first sentence as follows:

“Ferruginous lacustrine systems, such as Lake Towuti, Indonesia, represent specific cases of phosphorus cycling in which hydrous ferric iron (oxyhydr)oxides trap and precipitate phosphorus to the sediment, which reduces its bioavailability in the water column and thereby restricts primary production.”

- **line 34** is trivial. Also add “active” reduction on line 35 to make it also non-trivial. It is clear that the redox state is very low in this system to precipitate vivianite, the iron isotopes may suggest its active reduction in this zone. Be careful also with stating it is microbial reduction, as the isotope composition can be light also with abiotic reduction.

Answer 5: This sentence and rest of the abstract has been rewritten as follows:

“...Mineral inclusions like millerite and siderite reflect diagenetic mineral formation antecedent to the one of vivianite that is related to microbial reduction of iron and sulfate. Together with pore water profiles, these suggest that the precipitation of millerite, siderite, and vivianite in soft ferruginous sediments stems from the gradual microbial reduction of pore water electron acceptors. Based on solute concentrations and modeled mineral saturation indices, we inferred vivianite formation to initiate around 20 m depth in the sediment as the likely result of the decrease in microbial activity and associated P recycling in pore water. Negative $\delta^{56}\text{Fe}$ values of vivianite indicated incorporation of kinetically fractionated light Fe^{2+} into the crystals, likely derived from active reduction and dissolution of ferric oxides and transient ferrous phases during early diagenesis. The size and growth history of the nodules indicate that, after formation, continued growth of vivianite crystals constitutes a sink for P during burial, resulting in long-term P sequestration in ferruginous sediment.”

Introduction

I do not agree that vivianite is not a studied mineral in sediments. Please correct.

Answer 6: We removed “...less studied...” from the sentence.

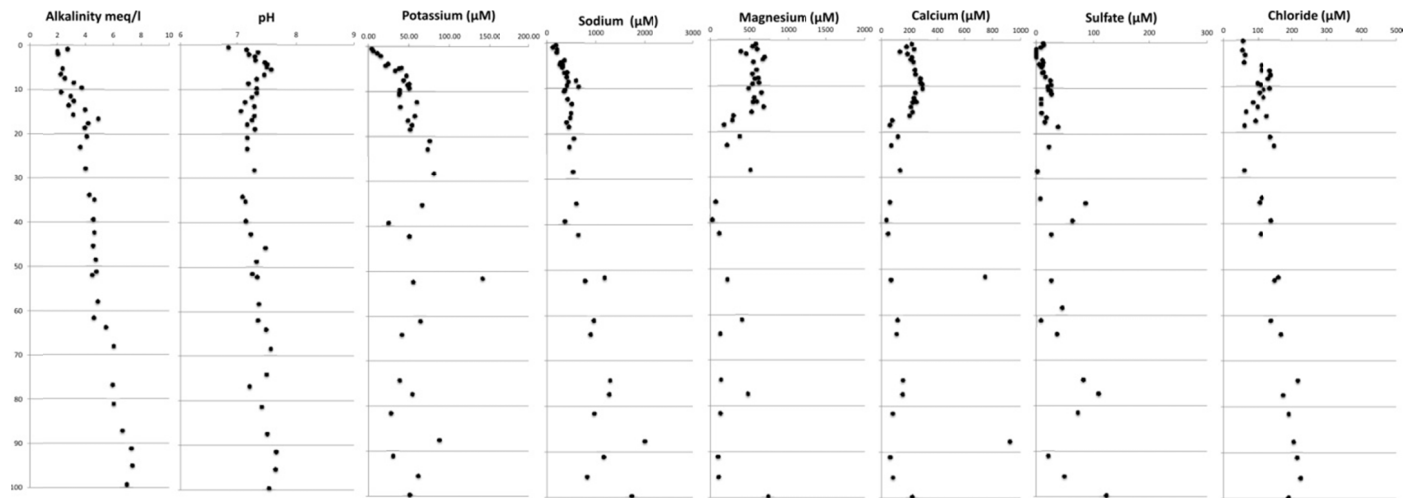
Methods

- **page 5:** Can the DIC be calculated indeed by this approach? How can the authors be sure the alkalinity is mostly carbonatic in this organic-rich sediment? Have they measured the carbonate alkalinity or the total alkalinity?

Answer 7: We measured total alkalinity along with the pH in pore water. In case, the relationship between total alkalinity and carbonate alkalinity according to Jenkins and Moore (1977) is the following:

$$\text{Carbonate alkalinity } (\text{CaCO}_3 \text{ mg/L}) = 100,000 [\text{K}_2(\text{HCO}_3^-)(10^{\text{pH}})].$$

We added the corresponding reference to the method part. We also measured pore water K^+ , Na^+ , Mg^{2+} , Ca^{2+} , SO_4^{2-} and Cl^- concentrations among others (here under, for information only) and checked the cation-anion mass balance. Thus, we are confident that the DIC calculated by this approach is consistent.



Additional reference:

- Jenkins, S. R., and Moore, R. C.: A proposed modification to the classical method of calculating alkalinity in natural waters, *J. Am. Water Works Ass.* 69: 56-60, <https://doi.org/10.1002/j.1551-8833.1977.tb02544.x>, 1977.

- **page 7:** I do not understand how the authors know that they isolate vivianite for the isotope measurement. Please clarify, also in consideration to the fact that diagenetic minerals are sometime more reactive to dissolution than detritus ones (refer to Henkel's publications).

Answer 8: Fe isotope analyses were carried out on entire vivianite crystals, not on pools obtained via Fe sequential extraction. We hand-picked vivianite crystals under the binocular from the dense mineral extracts. The separation and identification procedure is explained in part 2.4. These crystals were further used for XRD, SEM and TEM analyses, which resulted in the certain and definitive identification of the mineral vivianite. The same isolated vivianite crystals were processed for Fe isotope analyses. We clarified this in the text, for instance in:

- page 7, lines 9-10: "Minerals observed under a stereo microscope (Nikon SMZ800) included siderite, vivianite, millerite (i.e. NiS) and detrital pyroxene (i.e. Ca(Mg, Fe)Si₂O₆). Pyrite (i.e. FeS₂) was not observed. Vivianite crystals, which were identified in the interval from 20 to 50 m sediment depth, were hand-picked under the stereo microscope for further analyses."

-page 8, lines 17-19: "After density separation, vivianite crystals were hand-picked under the stereo microscope and the isolated crystals processed for Fe isotope analyses at the HELGES lab, GFZ Potsdam (von Blanckenburg et al., 2016); however, the presence of some minor inclusions of siderite, silicates and oxides within vivianite crystals could not be ruled out."

Discussion

- **page 12:** see also above. More data is needed and calculations to support precipitation of vivianite at the last glacial.

Answer 9: We do not state anywhere that vivianite crystallization initiated during the Last Glacial. We only provide the paleolacustrine context corresponding to the sediments that surround vivianite nodules and how

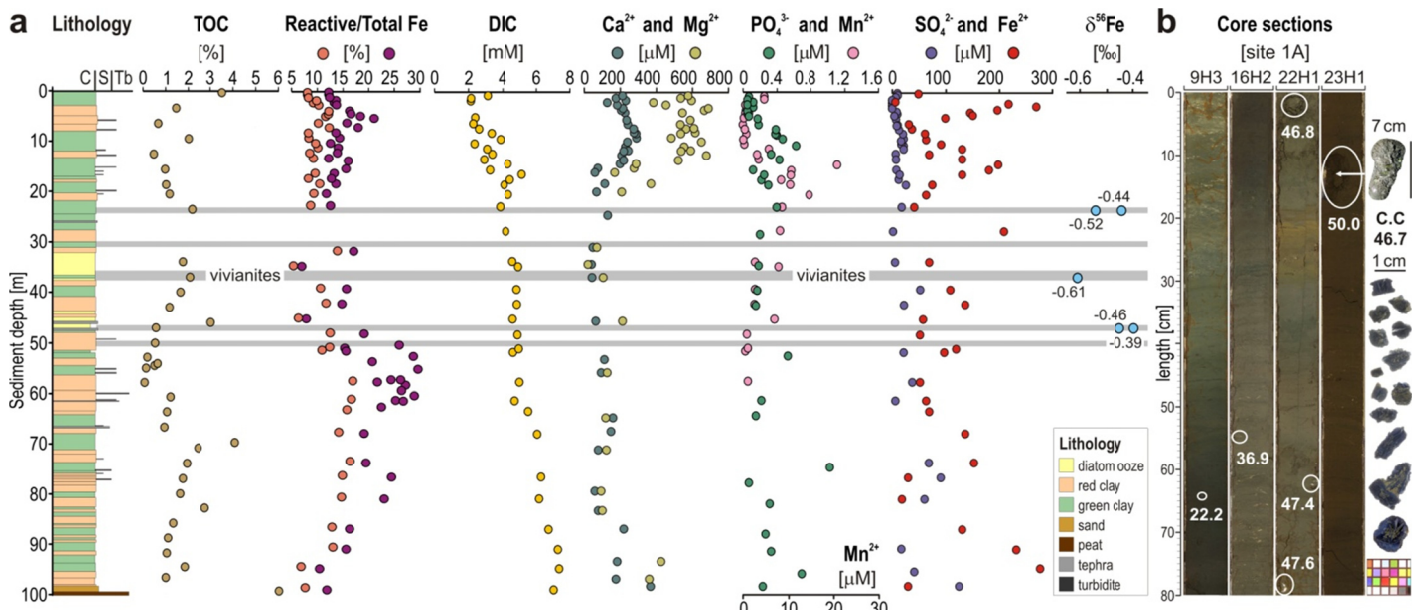
these sediments resulted in geochemical conditions that were favorable to the formation of vivianite during diagenesis, and thus later burial.

To clarify the link between lacustrine paleoconditions and post-depositional processes leading to the diagenetic formation of vivianite in this specific sedimentary interval, we modified the title and introductory sentences of this subchapter as follows:

“Past lacustrine conditions promoting vivianite formation during burial

In sulfur-poor, ferruginous settings, vivianite, siderite and magnetite can be formed in the sediments (Postma, 1981) depending on the local pH, CO_2 , PO_4^{3-} , the amount and reactivity of ferric oxides and OM buried in the sediment (Fredrickson et al., 1998; Glasauer et al., 2003; O’Loughlin et al., 2013). By analogy to hydromorphic soils (Maher et al., 2003; Vodyanitskii and Shoba, 2015), redox conditions at the time of deposition and fluxes of OM and reactive ferric oxides to the sediment would select for siderite or vivianite as the main diagenetic ferrous end-members during burial.”

Otherwise, we provide substantial additional pore water data (i.e. Ca^{2+} , Mg^{2+} , Mn^{2+} and SO_4^{2-} concentrations; see revised Figure 2) along with modeled saturation indices for siderite and vivianite (Table 1) to allow us to infer the initial depth of formation of vivianite (see answer no 3). In regards of these additional data, we have carefully checked and clarified the discussion.



Revised Figure 2

Additional references:

- Maher, B. A., Alekseev, A., and Alekseeva, T.: Magnetic mineralogy of soils across the Russian Steppe: climatic dependence of pedogenic magnetite formation. *Palaeogeogr. Palaeoclimatol. Palaeoecol.* 201, 321-341, doi: 10.1016/S0031-0182(03)00618-7, 2003.
- Vodyanitskii, Y. N., and Shoba, S. A.: Ephemeral $\text{Fe}(\text{II})/\text{Fe}(\text{III})$ layered double hydroxides in hydromorphic soils: A review, *Eurasian Soil Sci.*, 48, 240-249, doi: 10.1134/S10642293150, 2015.

- page 13: Again, also abiotic reduction can result in 2 ‰ fractionation.

Answer 10: We are aware of this fact. However, cases of abiotic reduction of Fe that reach 2 ‰ isotopic fractionation usually occur at oxic-anoxic interfaces (see Bullen et al., 2001; Wiesli et al., 2004; Wu et al., 2012). Pore waters are anoxic and it is unlikely that such abiotic fractionation could occur in the sediment. We provide multiple lines of evidence that vivianite crystals form in anoxic sediments, and not in the water column. Nevertheless, as answered to Reviewer 1, the second paragraph of section 4.3 was entirely rewritten to present Towuti's Fe mineralogy in terms of source to sink processes. We address the dissolution of initial and transient ferric/ferrous phases, the neoformation of minerals in the sediment and the related redistribution of Fe isotopes during reductive diagenesis. This includes potential abiotic fractionation at the water column oxycline. The second paragraph of section 4.3 has been rewritten as follows:

“...Compared to the global bulk igneous rock reservoir ($\delta^{56}\text{Fe} = +0.1 \pm 0.1 \text{ ‰}$) and ultramafic rocks (Dauphas et al. 2017) such as those present in Lake Towuti's catchment, the $\delta^{56}\text{Fe}$ measured on whole vivianite crystals (-0.61 to -0.39 ‰) reveals incorporation of isotopically fractionated light Fe^{2+} (Fig. 2a), even though traces of detrital iron-bearing minerals and secondary oxides are present within vivianite crystals (Figs 4 and 5). Towuti's Fe mineralogy from source to sink reflects complex cycling of Fe as iron minerals derived from catchment soils (e.g. goethite, hematite, magnetite) tend to transform into nanocrystalline Fe phases during reductive dissolution in the lake water column and sediment (Tamuntuan et al., 2015; Sheppard et al., 2019). Ferric/ferrous phases precipitating in equilibrium at the oxycline or during mixing events could be abiotically fractionated to 1-2 ‰ heavier/lighter isotope values than the remaining aqueous Fe^{2+} (Bullen et al., 2001; Skulan et al., 2002; Beard et al., 2010; Wu et al., 2011). After deposition, partitioning of the light Fe isotopes mainly transits through release to pore water (Henkel et al., 2016) implying a succession of mineral transformation and dissolution with internal diagenetic Fe redistribution during burial (Severmann et al., 2006; Scholz et al., 2014). For instance, mixed-valence iron oxides (e.g. green rust), which are authigenic phases that form initially under ferruginous conditions (Zegeye et al., 2012; Vuillemin et al., 2019a) are highly sorbent for pore water HCO_3^- and HPO_4^{2-} and can thereby transform into either siderite or vivianite as the sediment ages (Hansen and Poulsen, 1999; Bocher et al., 2004; Refait et al., 2007; Halevy et al., 2017). Because vivianite formation initiates in the sediment, we infer that vivianite crystals acted as additional traps for the reduced Fe^{2+} released to pore water and that their light $\delta^{56}\text{Fe}$ values are consistent with kinetic fractionation related to microbial Fe reduction during early diagenesis, or eventually inherited from post-depositional dissolution of transient ferrous phases. In the latter case, pre-depositional processes of abiotic Fe fractionation related to stratified conditions will require further investigations...”

Additional references:

- Bocher, F., Géhin, A., Ruby, C., Ghanbaja, J., Abdelmoula, M., and Génin, J.-M. R.: Coprecipitation of Fe(II–III) hydroxycarbonate green rust stabilized by phosphate adsorption, *Solid State Science*, 6, 117–124, <https://doi.org/10.1016/j.solidstatesciences.2003.10.004>, 2004.
- Brantley, S. L., Liermann, L., and Bullen, T. D.: Fractionation of Fe isotopes by soil microbes and organic acids, *Geology*, 29, 535–538, [https://doi.org/10.1130/0091-7613\(2001\)029<0535:FOFIBS>2.0.CO;2](https://doi.org/10.1130/0091-7613(2001)029<0535:FOFIBS>2.0.CO;2), 2001.
- Bullen, T. D., White, A. F., Childs, C. W., Vivit, D. V., & Schulz M. S. Demonstration of significant abiotic iron isotope fractionation in nature. *Geology* 29, 699–702 (2001).

- Halevy, I., Alesker, M., Schuster, E. M., Popovitz-Biro, R., and Feldman, Y.: A key role for green rust in the Precambrian oceans and the genesis of iron formations, *Nat. Geosci.*, 10, 135–139, <https://doi.org/10.1038/ngeo2878>, 2017.
- Hansen, H. C. B., and Poulsen, I. F.: Interaction of synthetic sulphate "green rust" with phosphate and the crystallization of vivianite, *Clay. Clay Miner.*, 47, 312-318, doi: 10.1346/CCMN.1999.0470307, 1999.
- Henkel, S., Kasten, S., Poulton, S. W., and Staubwasser, M.: Determination of the stable iron isotopic composition of sequentially leached iron phases in marine sediments. *Chem. Geol.* 421, 93-102, <https://doi.org/10.1016/j.chemgeo.2015.12.003>, 2015.
- Refait, P., Reffass, M., Landoulsi, J., Sabot, R., and Jeannin, M.: Role of phosphate species during the formation and transformation of the Fe(II-III) hydroxycarbonate green rust, *Colloid. Surface A.*, 299, 29–37, doi: 10.1016/j.colsurfa.2006.11.013, 2007.
- Scholz, F., Severmann, S., McManus, J., Noffke, A., Lomnitz, U., and Hensen, C.: On the isotope composition of reactive iron in marine sediments: Redox shuttle versus early diagenesis. *Chem. Geol.*, 389, 48-59, <https://doi.org/10.1016/j.chemgeo.2014.09.009>, 2014.
- Severmann, S., Johnson, C. M., Beard, B. L., and McManus, J.: The effect of early diagenesis on the Fe isotope compositions of porewaters and authigenic minerals in continental margin sediments, *Geochim. Cosmochim. Ac.*, 70, 2006-2022, <https://doi.org/10.1016/j.gca.2006.01.007>, 2006.
- Welch, S. A., Beard, B. L., Johnson, C. M., & Braterman, P. S. Kinetic and equilibrium Fe isotope fractionation between aqueous Fe(II) and Fe(III). *Geochim. Cosmochim. Ac.* **67**, 4231-4250 (2003).
- Wiesli, R. A., Beard, B. L., & Johnson, C. M. Experimental determination of Fe isotope fractionation between aqueous Fe(II), siderite and "green rust" in abiotic systems. *Chem. Geol.* **211**, 343-362 (2004).
- Wu, L., Percak-Dennett, E. M., Beard, B. L., Roden, E. E., & Johnson, C. M. Stable iron isotope fractionation between aqueous Fe(II) and model Archean ocean Fe-Si coprecipitates and implications for iron isotope variations in the ancient rock record. *Geochim. Cosmochim. Ac.* **84**, 14-28 (2012).

Reviewer 3

We thank the Reviewer for his/her positive and careful review of our manuscript, which highly helped us improving the new version of the manuscript presently submitted. We have addressed all of the Reviewer's concerns with additional data, namely:

- Downcore profiles for both highly reactive and total iron in bulk sediment.
- Pore water SO_4^{2-} , Ca^{2+} , Mg^{2+} and Mn^{2+} concentrations were added to Figure 2a and are discussed in the revised manuscript.
- Based on geochemical modeling of pore water major ions, we calculated saturation indices for specific minerals (e.g. vivianite, siderite). These indices are listed in a new table (Table 1) now included in the revised manuscript.

We did our best to fulfill all the remarks and suggestions brought by the Reviewer. Each comment has been addressed in separate answers, and all the corresponding changes are highlighted in red in the text. Please, find here after our point by point answers to Reviewer 3.

Yours sincerely,
Aurèle Vuillemin

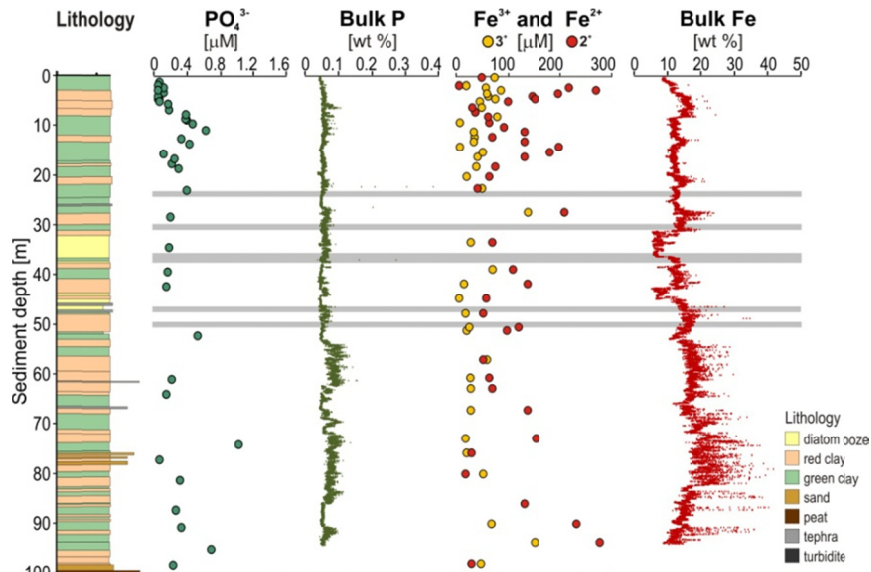
General comments

- **Comment 1:** In my opinion, the impact of the paper could increase by adding an implications section at the end of the discussion. Here the authors could present a mass balance for P and discuss the importance of vivianite in the burial of P in this and other lake sediments. Now it is only briefly mentioned that vivianite might act as the main sink for P (page 11, line 31).

Answer 1: We do not have sufficient quantitative measurements of P concentrations and vivianite crystals in bulk sediment to accurately model the P mass balance. To satisfy the Reviewer's interest, we provide at his/her discretion preliminary XRF profiles (here under) and compare them with those of pore water. We are reluctant to provide XRF data for publication or discuss them any further since they are not calibrated and are part of another manuscript in preparation.

To address the relevance of vivianite in P burial, we oriented the discussion around saturation indices modeled for vivianite and siderite (Table 1), and show how pore water saturation with respect to vivianite increases with depth and leads to the gradual depletion of dissolved phosphate with burial.

We further discuss P cycling in the present ferruginous analogue and compare pore water concentrations to those interpreted from the Archean rock record. We added a short paragraph at the end of the discussion summing up the implications of P cycling processes in modern ferruginous sediment and use those interpretations from the rock record of Archean marine sediments (see answer no. 2).



Preliminary XRF profiles

5 m depth	Saturation	10 m depth	Saturation
talc	1.43	siderite	1.00
siderite	1.29	quartz	0.71
quartz	0.71	vivianite	-0.04
vivianite	-0.45	talc	-0.31
calcite	-0.68	calcite	-0.83
dolomite	-0.77	aragonite	-0.97
aragonite	-0.82	dolomite	-1.27

Table 1

- **Comment 2:** The authors mention in the abstract and introduction that Lake Towuti can be used as an analogue for the Archean ocean. However in the discussion, I miss the implications that this study has for the Archean ocean.

Answer 2: We added a paragraph at the end of the discussion summing up the implications of the diagenetic processes observed in modern ferruginous sediment for the Archean oceans as interpreted from the ancient rock record. This paragraph reads as follows:

“Whether they relate to microbial reduction in soft ferruginous sediment or past conditions in bottom waters, biotic and abiotic diagenetic processes remain challenging to constrain in terms of ancient rock record (Johnson et al., 2013). Concentrations estimates for deep anoxic waters interpreted from the Archean rock record typically range from 40 to 120 μM for Fe and 0.1 to 0.3 μM for P (Holland, 2006; Konhauser et al., 2007; Jones et al., 2015), which are similar to those presently observed in the pore water of ferruginous analogue Lake Towuti (Fig. 2a). Concerning P diagenesis, it is hypothesized that P availability in the Archean ocean was limited by the lack of terminal electron acceptors and oxidative power used to recycle most of the OM-bound P rather than by scavenging by Fe minerals (Kipp and Stüeken, 2017; Michiels et al., 2017; Herschy et al., 2018). The present Ca^{2+} and Mg^{2+} concentrations in pore water exert apparent control

on the precipitation of siderite and/or vivianite during early diagenesis (Vuillemin et al., 2019a), which is comparable to interpretations of ancient P availability in regards to hydrothermal and continental weathering of mafic rocks (Jones et al., 2015). In this context because secondary P-bearing minerals cannot form if P remains bound to OM, we suggest that the precipitation of millerite, siderite, and vivianite in the sediment constitute a likely diagenetic sequence stemming from the depletion of pore water electron acceptors and related loss of oxidative power during OM remineralization, with consequent long-term P sequestration.”

Additional references:

- Herschy, B., Chang, S. J., Blake, R., Lepland, A., Abbott-Lyon, H., Sampson, J., Atlas, Z., Kee, T. P., and Pasek, M. A.: Archean phosphorus liberation induced by iron redox geochemistry, *Nat. Commun.*, 9, 1346, <https://doi.org/10.1038/s41467-018-03835-3>, 2018.
- Kipp, M. A., and Stüeken, E. E.: Biomass recycling and Earth’s early phosphorus cycle, *Sci. Adv.*, 3, eaao4795, <https://doi.org/10.1126/sciadv.aao4795>, 2017.
- Konhauser, K. O., LaLonde, S. V., Amskold, L., and Holland, H. D.: Was there really an Archean phosphate crisis?, *Science*, 315, 1234, <https://doi.org/10.1126/science.1136328>, 2007.
- Michiels C.C., Darchambeau, F., Roland, F. A., Morana, C., Llirós, M., Garcia-Armisen, T., Thamdrup, B., Borges, A. V., Canfield, D. E., Servais, P., Descy, J.-P., and Crowe, S. A.: Iron-dependent nitrogen cycling in a ferruginous lake and the nutrient status of Proterozoic oceans, *Nat. Geosci.*, 10, 217-221, <https://doi.org/10.1038/NGO2886>, 2017.

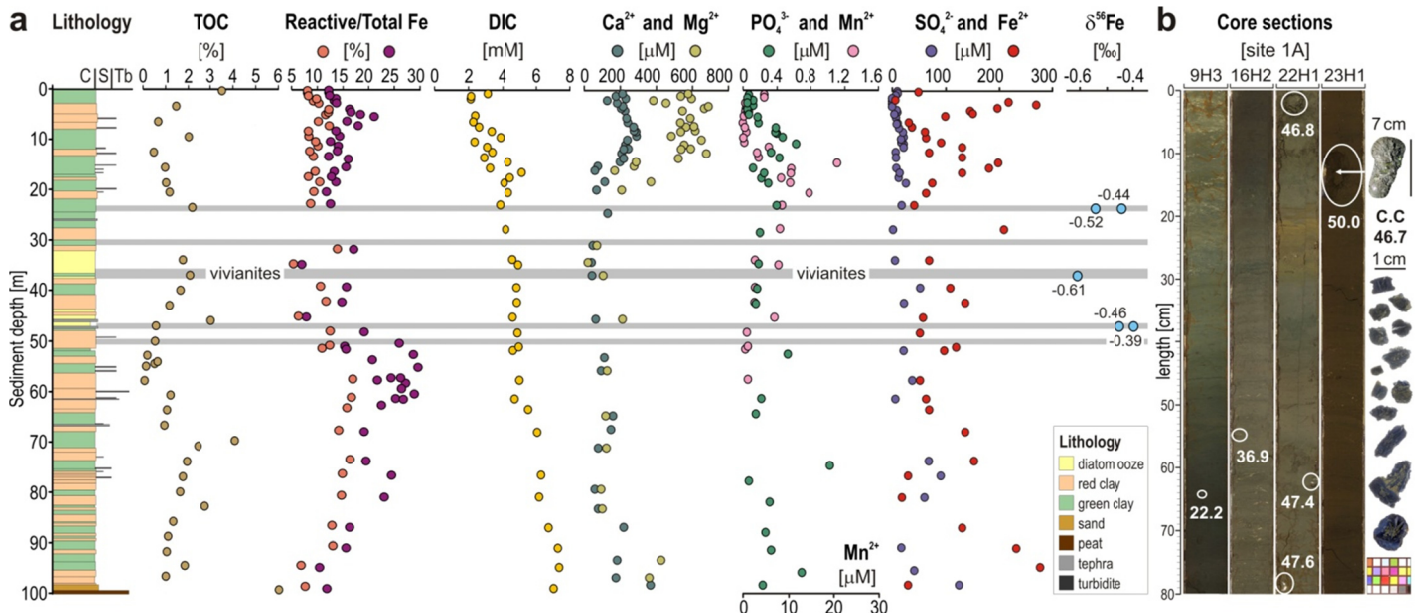
- **Comment 3:** I would like to also see the Fe extraction data for this core. It is mentioned in the method section that Fe extractions were carried out, however they are now only used to calculate the total Fe present.

Answer 3: Because sequential Fe extractions constitute the main part of a manuscript presently in preparation, we refrain from providing the complete dataset. To satisfy the Reviewer’s legitimate comment, we provide downcore profiles for the highly reactive Fe (i.e. the sum of four successive Fe pools) and total Fe (i.e. reactive + non-reactive) pools in the revised Figure 2a.

We clarified the extraction procedure in the method section, part 2.2, and cite the corresponding manuscript available as preprint at <https://www.EarthArXiv.org>. We also updated Figure 2a (here under) and complemented the results, part 3.2, accordingly.

Additional reference:

- Bauer, K. W., Byrne, J., Kenward, P., Simister, R., Michiels, C., Friese, A., Vuillemin, A., Henny, C., Nomosatryo, S., Kallmeyer, J., Kappler, A., Smit, M., Francois, R., Crowe, S. A.: Magnetite biomineralization in ferruginous waters and early Earth evolution, *EarthArXiv Preprint*, <https://doi.org/10.31223/osf.io/prhuz>, 2020.



Revised Figure 2

Specific comments

Introduction

- page 2, line 8: “under anoxia”. Here reducing conditions are also important, not only anoxic conditions.

Answer 4: Rephrased to “...reducing conditions and long-term anoxia...”

- line 8: “..phosphate..”. Phosphate should be phosphorus (or P) in this case.

Answer 5: Modified accordingly.

- line 10: This is only the case when there is sufficient organic matter, otherwise there is no formation of sulfide and eventually Fe sulfides.

Answer 6: Modified accordingly to “....high sulfate (SO_4^{2-}) concentrations and sufficient labile OM,...leads to the formation of sulfides and eventually iron sulfides that decrease...”

- line 12: “Formation of iron phosphate minerals..”. Mention that these are reduced iron phosphate minerals.

Answer 7: Mentioned accordingly.

- line 22: “In such systems..” Besides the presence of P also the rate/amount of Fe reduction is important in oligotrophic environments. When the organic matter content is low this can lead to limited Fe reduction, low concentrations of pore water Fe and limited formation of vivianite. This has recently been shown in a modeling study for an oligotrophic estuary in the Bothnian Sea (Lenstra et al., 2018)

Answer 8: We added the following sentence to the text:

“Besides P concentrations, low content and reactivity of OM may also narrow rates of Fe reduction and thereby preclude vivianite formation due to limited release of Fe^{2+} to pore water (Lenstra et al., 2018).”

We added (Lenstra et al., 2018) to the list of references and cite it where appropriate in the manuscript.

- **line 27:** (Egger et al., 2015; Dijkstra et al., 2016) show vivianite formation in brackish (not marine) environments. The formation of vivianite, when there is sufficient organic matter, is sensitive to the production of sulfide in the sediment. So at a higher salinity (enhanced sulfide production) the formation of vivianite is expected to be lower. The dependence of vivianite formation on salinity is also discussed in the modeling study by (Lenstra et al., 2018).

Answer 9: Thank you for this correction. We replaced “marine” by “brackish” in the corresponding sentence. We also added one sentence to clarify the influence of salinity and OM content on sulfide production in the sediment:

“However, high salinities and substantial burial of OM can promote microbial reduction of SO_4^{2-} and sulfide production, which tend to restrict the formation of vivianite in the sediment (Lenstra et al., 2018).”

- **page 3, line 22:** “...is stable under anoxic conditions..” Add that it is also important to have non-sulfidic conditions. (anoxic/non sulfidic).

Answer 10: Modified accordingly.

Section 2.3

- **page 5, line 2:** In these steps, you do not extract Fe present in pyrite. I guess this is a very small pool in these environments but to correctly determine the HR Fe pool this should be included or mentioned that this is not included.

Answer 11: We added the following information in the methods, part 2.2.:

“For reactive and total Fe sequential extraction, we processed 200 mg of sediment according to Poulton and Canfield (2005). The highly reactive Fe pool is defined as the sum of carbonate-associated Fe (acetate extractable Fe), hydrous Fe (oxyhydr)oxides including ferrihydrite and lepidocrocite (0.5 N HCl extractable Fe), ferric (oxyhydr)oxides including hematite and goethite (dithionite extractable Fe), and magnetite (oxalate extractable Fe). These reagents do not extract the Fe present in pyrite (Henkel et al., 2016). The non-reactive Fe pool is defined as Fe contained in silicate minerals after removal of reactive phases (near boiling 6N HCl extractable Fe). Total Fe was obtained by summing up the highly reactive Fe pools and the non-reactive Fe contained in silicate minerals (Bauer et al., 2020).”

- **line 2:** How is the non-reactive Fe fraction determined?

Answer 12: The non-reactive Fe pool is defined as the Fe contained in silicate minerals after removal of reactive phases (near boiling 6N HCl extractable Fe). See answer 11.

Section 2.4

- **line 13:** Was this carried out under anoxic conditions?

Answer 13: Yes, all pore water extractions were carried out in an anaerobic chamber. This was already mentioned in part 2.1:

“Pore water was extracted on site from 5-cm-long whole round cores (6.6 cm diameter) that were cut from the core sections, immediately capped and transferred to an anaerobic chamber flushed with nitrogen to avoid oxidation during sample handling (Friese et al., 2017).”

We now mention this once more in part 2.3: “After transfer of the whole round cores to the anaerobic chamber, pore water within the upper ten meters was extracted using Rhizon...”

Section 2.5

- **page 6, line 6:** “Below and above this interval, vivianites are rarely present in the sediment, which was confirmed by smear slide analysis (Russell et al., 2016) and X-ray diffraction (Supplementary Fig. S2).” This should be moved to the discussion section.

Answer 14: Moved accordingly to the discussion, part 4.2 (page 14, line 10).

Section 3.2

It would be interesting if you can also show your Fe extraction results in this section. Maybe in the appendix, if you don't want to add an additional figure to the manuscript.

Answer 15: Please refer to answers no. 3, 11 and 12.

Section 4.1

- **page 11, line 24:** Is it possible that the orientation of the mineral in the sediment changed during coring? I wonder because the mineral is located very close to the core liner.

Answer 16: Although sediment disturbance cannot be fully excluded, we observed multiple vivianites in different core sections, with crystal orientation reflecting an upward growth (Supplementary Fig. S5) so that polarity and growth direction can be inferred without difficulty.

- **line 27:** Would it be possible to include the solid phase Fe speciation in the paper?

Answer 17: See answers no. 3, 11, 12 and 15

- **line 30:** But concentrations of phosphate are generally low not only at places where vivianite is found. I would therefore, based on only the phosphate data, not suggest that vivianite is the main sink of P.

Answer 18: Rephrased from “...acted as a main P sink...” to “...could act as a P sink from the pore water to the sediment during diagenesis”.

- **page 12, line 10:** Here and elsewhere Potsma should be Postma

Answer 19: Corrected accordingly.

- **line 11:** “..depending on the local pH, CO_2 , PO_4^{3-} , and the amount of reactive ferric oxides buried..”. Here, also the amount and reactivity of organic matter is important.

Answer 20: This was added to the sentence accordingly.

Conclusions

- **page 13, line 5:** I do not understand what partially dissolved iron oxides are.

Answer 21: Rephrased to “...partially dissolved goethite...”

Microbially mediated formation of vivianite during early diagenesis in ferruginous sediments, Lake Towuti, Indonesia.

Aurèle Vuillemin^{1,2}, André Friese¹, Richard Wirth¹, Jan A. Schuessler¹, Anja M. Schleicher¹, Helga Kemnitz¹, Andreas Lücke³, Kohen W. Bauer^{4,5}, Sulung Nomosatryo^{1,6}, Friedhelm von Blanckenburg¹,
5 Rachel Simister⁴, Luis G. Ordoñez⁷, Daniel Ariztegui⁷, Cynthia Henny⁶, James M. Russell⁸, Satria Bijaksana⁹, Hendrik Vogel¹⁰, Sean A. Crowe^{4,5,11}, Jens Kallmeyer¹ and the Towuti Drilling Project Science Team*.

¹GFZ German Research Centre for Geosciences, Helmholtz Centre Potsdam, Potsdam, 14473, Germany

²Present address: Department of Earth and Environmental Science, Paleontology and Geobiology, Ludwig-Maximilians-10 Universität München, Munich, 80333, Germany

³Research Center Jülich, Institute of Bio- and Geosciences 3: Agrosphere, Jülich, 52428, Germany

⁴Department of Earth, Ocean, and Atmospheric Sciences, University of British Columbia, Vancouver, BC, V6T 1Z4, Canada

⁵Present address: Department of Earth Sciences, University of Hong Kong, Hong Kong, China

⁶Research Center for Limnology, Indonesian Institute of Sciences (LIPI), Cibinong-Bogor, Indonesia

¹⁵7Department of Earth Sciences, University of Geneva, Geneva, 1205, Switzerland

⁸Department of Earth, Environmental, and Planetary Sciences, Brown University, 13 Providence, RI, 02912, USA

⁹Faculty of Mining and Petroleum Engineering, Institut Teknologi Bandung, 15 Bandung, 50132, Indonesia

¹⁰Institute of Geological Sciences and Oeschger Centre for Climate Change Research, University of Bern, CH-3012, Bern, Switzerland

²⁰¹¹Department of Microbiology and Immunology, University of British Columbia, Vancouver, BC, V6T 1Z3, Canada

*A full list of authors appears at the end of the paper

Correspondence to: Aurèle Vuillemin (a.vuillemin@lrz.uni-muenchen.de)

Abstract. Ferruginous lacustrine systems, such as Lake Towuti, Indonesia, represent specific cases of phosphorus cycling in which hydrous ferric iron (oxyhydr)oxides trap and precipitate phosphorus to the sediment, which reduces its bioavailability 25 in the water column and thereby restricts primary production. The oceans were also ferruginous during the Archean, so understanding the dynamics of phosphorus in modern-day ferruginous analogues may shed light on the marine biogeochemical cycling that dominated much of Earth's history. Here we report the presence of large crystals (>5 mm) and nodules (>5 cm) of vivianite – a ferrous iron phosphate – in sediment cores from Lake Towuti, and address the processes of 30 vivianite formation, phosphorus retention by iron and the related mineral transformations during early diagenesis in ferruginous sediments.

Core scan imaging together with analyses of bulk sediment and pore water geochemistry document a 30 m long interval consisting of sideritic and non-sideritic clayey beds and diatomaceous oozes containing vivianites. High-resolution imaging of vivianite revealed continuous growth of crystals from tabular to rosette habits that eventually form large (up to 7 cm) vivianite nodules in the sediment. Mineral inclusions like millerite and siderite reflect diagenetic mineral formation 35 antecedent to the one of vivianite that is related to microbial reduction of iron and sulfate. Together with pore water profiles, these suggest that the precipitation of millerite, siderite, and vivianite in soft ferruginous sediments stems from the gradual

microbial reduction of pore water electron acceptors. Based on solute concentrations and modeled mineral saturation indices, we inferred vivianite formation to initiate around 20 m depth in the sediment as the likely result of the decrease in microbial activity and associated P recycling in pore water. Negative $\delta^{56}\text{Fe}$ values of vivianite indicated incorporation of kinetically fractionated light Fe^{2+} into the crystals, likely derived from active reduction and dissolution of ferric oxides and transient ferrous phases during early diagenesis. The size and growth history of the nodules indicate that, after formation, continued growth of vivianite crystals constitutes a sink for P during burial, resulting in long-term P sequestration in ferruginous sediment.

1 Introduction

In the lacustrine realm, phosphorus (P) is often the limiting nutrient for primary production (Compton et al., 2000). Its supply to primary producers in the euphotic zone depends on external fluxes (Manning et al., 1999; Zegeye et al., 2012) and internal recycling as a result of organic matter (OM) mineralization in both the water column and underlying sediments (Katsev et al., 2006; Hupfer and Lewandowski, 2008). Removal of P through burial in sediments depends partly on sorption to iron oxides (Wilson et al., 2010), and because iron oxides tend to dissolve under reducing conditions and long-term anoxia, phosphate burial is sensitive to the oxygenation state of the water column and water-sediment interface (Sapota et al., 2006; Rothe et al., 2015). In environments with high sulfate (SO_4^{2-}) concentrations and sufficient labile OM, microbial SO_4^{2-} reduction usually leads to the formation of sulfides and eventually iron sulfides, that decrease Fe-recycling and the formation of Fe (oxyhydr)oxides in the upper oxygenated sediments, and this in turn decreases the extent to which P is retained in the sediment (Roden and Edmonds, 1997). Formation of iron phosphate minerals such as vivianite (i.e. $\text{Fe}_3(\text{PO}_4)_2 \cdot 8\text{H}_2\text{O}$) in response to the accumulation of sedimentary Fe and P (Gächter et al., 1988; Wilson et al., 2010; Rothe et al., 2016) is a process that, in contrast, can contribute to long-term P retention in the sediment, particularly in ferruginous (anoxic, non-sulfidic) environments (Gächter and Müller, 2003). Although anoxia is commonly thought to promote P release from sediments and its recycling back to the photic zone of the water column, the high ferrous iron concentrations that can develop in ferruginous environments may promote the formation of iron phosphate minerals, thereby restricting P recycling and bioavailability.

Vivianite is a common phosphate mineral in lacustrine systems (Vuillemin et al., 2013; Rothe et al., 2015). It regularly occurs in organic-rich sediments, often in close association with macroscopic organic remains, and when production of sulfide is low (Rothe et al., 2016). Although it is common in eutrophic lakes, presumably due to high P concentrations, its occurrence in ferruginous, oligotrophic lakes, which may be similar to the Archean oceans, is poorly known. In such systems, high Fe concentrations should catalyze vivianite formation, yet low P concentrations may preclude its formation.

Besides P concentrations, low content and reactivity of OM may also narrow rates of Fe reduction and thereby preclude vivianite formation due to limited release of Fe^{2+} to pore water (Lenstra et al., 2018).

As reported from laboratory studies, vivianite nucleation is possible under relatively high concentrations of Fe^{2+} and orthophosphate (solubility product: $K_{\text{sp}} = 10^{-36}$) at pH between 6 and 9 (Glasauer et al., 2003; Rothe et al., 2014; Sánchez-Román et al., 2015). It thus forms as a secondary mineral product in response to iron reduction when P concentrations are sufficiently high (Fredrickson et al., 1998; Zachara et al., 1998; O'Loughlin et al., 2013). Despite these requirements, 5 vivianite formation is not restricted to any specific lake trophic state or salinity range and has been shown to form under a broad range of bottom water redox conditions in freshwater to brackish environments (Egger et al., 2015; Dijkstra et al., 2016). However, high salinities and substantial burial of OM can promote microbial reduction of SO_4^{2-} and sulfide production, which tend to restrict the formation of vivianite in the sediment (Lenstra et al., 2018).

In the humid tropics, deep and intense chemical weathering of bedrock often leads to the formation of thick laterite soils 10 residually enriched in iron (oxyhydr)oxides that promote P scavenging (Lemos et al., 2007). Erosion of these soils and subsequent delivery to lakes promotes P deposition and retention in lake sediments (Fagel et al., 2005; Sapota et al., 2006; Rothe et al., 2014). One of such environment is the ancient Malili Lake System, Sulawesi, Indonesia (Lehmuusluoto et al., 1995; Haffner et al., 2001), whose catchment is dominated by ultramafic bedrock overlain by thick lateritic soils (Golightly et al., 2010; Morlock et al., 2019). The Malili Lakes are presently characterized by a dearth of SO_4^{2-} (Crowe et al., 2004; 15 Vuillemin et al., 2016) and low biomass (Bramburger et al., 2008), likely because fluxes of iron (oxyhydr)oxides from surrounding soils scavenge P in the soils, rivers and lake surface waters (Crowe et al., 2008; Katsev et al., 2010; Zegeye et al., 2012). In Lake Towuti, environmental and sedimentary processes, such as weathering intensity (Russell et al., 2014; 20 Morlock et al., 2019), lake mixing and bottom water oxygenation (Costa et al., 2015), and fluctuations in lake level and deltaic sedimentation (Vogel et al., 2015; Hasberg et al., 2019) have changed through time and altered the abundance of reactive ferric iron, and potentially P, in the water column and sediment. However, P dynamics have not been intensively studied in this lake.

On the short term, P retention in lake sediments mainly depends on the oxygenation of the water column (Reed et al., 2016), 25 with depletion of the reducible iron pool under oxygen-poor conditions resulting in the release of accumulated P from the sediment (Katsev et al., 2006). For instance in 600 m deep permanently stratified Lake Matano (Crowe et al., 2008), microbial reduction of iron, which takes place below the modern-day oxycline, leads to partial release of adsorbed P into the bottom water and its accumulation over time (Crowe et al., 2008). Like Lake Matano, Lake Towuti, the largest of the Malili Lakes, presently displays an extreme scarcity of SO_4^{2-} ($<20 \mu\text{M}$), nitrate/nitrite ($<5 \mu\text{M}$), phosphate ($\text{PO}_4^{3-} <5 \mu\text{M}$) and oxygen depletion below ~ 130 m water depth (Vuillemin et al., 2016). Evidence for a complete overturn of the water column is absent in recent years, but sediment data indicate that periods of complete overturn and bottom water oxygenation may 30 have occurred in the geological past (Costa et al., 2015). In an oxygenated water column, hydrous ferric oxides could reach the water-sediment interface and prevent P and Fe release from the sediment (Shaffer, 1986; Katsev et al., 2006). In contrast, anoxia should favor the release of P and Fe from surface sediments and pore waters back to the anoxic bottom water, which would fundamentally change the lake's biology. Even though the lake is presently stratified, PO_4^{3-} in the modern anoxic lake is extraordinarily low, implying a sink for P that is stable under anoxic non-sulfidic conditions, like vivianite. Sediment drill

core data, furthermore, indicate that Lake Towuti has undergone large changes in primary productivity through time, suggesting very different P biogeochemical cycling in the past, possibly linked to dynamics in sediment P mineralogy.

The Malili Lakes, including Lake Towuti, thus represent a relevant setting in which to explore the distribution and characteristics of vivianite formed under Fe-rich and fluctuating redox conditions. From May to July 2015, the Towuti

5 Drilling Project (TDP) recovered more than 1000 m of sediment drill core from three sites in Lake Towuti, including a 113-m-long core dedicated to geomicrobiological studies at site TDP-TOW15-1A (Russell et al., 2016; Friese et al., 2017). The discovery of sedimentary beds containing large vivianite crystals in this core prompted the present study investigating the distribution and characteristics of vivianite and the modes of vivianite formation in response to environmental variability, P sorption processes and early diagenesis of iron phases.

10 2 Methods

2.1 Study site and drilling operations

Lake Towuti (2.5°S, 121°E) is a 200 m deep lake that is part of the Malili Lake System (Fig. 1), a chain of five interconnected tectonic lakes seated in ophiolitic rocks covered with thick lateritic soils on Sulawesi Island, Indonesia (Lehmuusluoto et al., 1995; Haffner et al., 2001). The Mahalona River, which is Lake Towuti's main inflow to the north,

15 connects to the upstream Lakes Mahalona and Matano, while the Larona River constitutes Lake Towuti's only outflow to the west (Vogel et al., 2015). Lake Towuti's water column is circumneutral (pH = 8.4 to 7.2), weakly thermally stratified (i.e. 31–28°C) and presently oxygen-depleted below ~130 m depth (Nomosatryo et al., 2013). The water chemistry is dominated by Mg²⁺ and HCO₃⁻ ions (Lehmuusluoto et al., 1995; Haffner et al., 2001).

The TDP coring operations were carried out from May to July 2015 using the International Continental Scientific Drilling

20 Program (ICDP) Deep Lakes Drilling System (Russell et al., 2016). Hole TDP-TOW15-1A (156 m water depth; hereafter TDP-1A) was drilled in May 2015 with a fluid contamination tracer used to aid geomicrobiological sampling and analysis (Friese et al., 2017). Samples were collected from cores from TDP-1A immediately upon recovery and over 450 samples were subsequently processed in the field for analyses of pore-water chemistry, cell counting and microbial fingerprinting, and organic geochemistry.

Pore water was extracted on site from 5-cm-long whole round cores (6.6 cm diameter) that were 25 cut from the core sections, immediately capped and transferred to an anaerobic chamber flushed with nitrogen to avoid oxidation during sample handling (Friese et al., 2017). Core catchers from TDP-1A were packed into gas-tight aluminum foil bags flushed with nitrogen gas and heat-sealed to keep them under anoxic conditions until mineral extraction. In January

2016, the unsampled remainders of the cores from TDP-1A were split and scanned at the Limnological Research Center, Lacustrine Core Facility (LacCore), University of Minnesota, described macroscopically and microscopically to determine

30 their stratigraphy and composition (Russell et al., 2016) and then subsampled. Minerals from core catcher sediments were extracted after 3 month of storage, and macroscopically visible vivianite crystals were hand-picked from split TDP-1A cores after 8 months of storage. Except as otherwise noted, all our samples and measurements come primarily from hole TDP-1A.

2.2 Total organic carbon, reactive and total iron

Sediment from core catchers from TDP-1A was used to quantify total organic carbon (TOC). Sediment samples were freeze-dried prior to analysis. Carbonate minerals were removed by treating the samples with 20 mL of 5 % HCl at 50° C for 24 hours (Golubev et al., 2009). Following treatment, samples were repeatedly rinsed with deionized water to reach neutral pH, 5 centrifuged to discard water and freeze-dried. We tested this treatment using 200 mg of technical grade siderite (FeCO_3) to evaluate dissolution. Results showed that 85 % of the siderite is efficiently dissolved within the first 2 hours of treatment and 95 to 100 % after 24 hours (Supplementary Fig. S1). About 8 to 10 mg of homogenized decarbonated samples were measured using an elemental analyzer (EuroVector, EuroEA). Combustion was done in an excess of oxygen at 1040 °C. TOC concentrations were calculated from the yield of CO_2 after sample combustion in the elemental analyzer. Analytical 10 precision of the method is $\pm 3\%$ (1σ) of the yield of CO_2 . TOC was recalculated to the content of the whole sample and results are presented in dry mass weight % (wt %).

For reactive and total Fe sequential extraction, we processed 200 mg of sediment according to Poulton and Canfield (2005). The highly reactive Fe pool is defined as the sum of carbonate-associated Fe (acetate extractable Fe), hydrous Fe (oxyhydr)oxides including ferrihydrite and lepidocrocite (0.5 N HCl extractable Fe), ferric (oxyhydr)oxides including 15 hematite and goethite (dithionite extractable Fe), and magnetite (oxalate extractable Fe). These reagents do not extract the Fe present in pyrite (Henkel et al., 2016). The non-reactive Fe pool is defined as Fe contained in silicate minerals after removal of reactive phases (near boiling 6N HCl extractable Fe) (Bauer et al., 2020). Total Fe was obtained by summing up the highly reactive Fe pools and the non-reactive Fe contained in silicate minerals. Our protocol could dissolve $>92\%$ of the Fe from the PACS-2 international reference standard, ensuring high Fe yield from the samples. All Fe concentration 20 measurements were performed using a Varian AA875 Flame Atomic Absorption Spectrophotometer (Varian, Palo Alto, USA). Precision on triplicate measurements was 1.2 % and our limit of detection was $1500 \mu\text{g g}^{-1}$ (0.15 wt % or $\sim 10 \mu\text{mol cm}^{-3}$).

2.3 Pore water geochemistry

After transfer of the whole round cores to the anaerobic chamber, pore water within the upper ten meters was extracted 25 using Rhizon Pore Water Samplers (Rhizosphere research products, Dolderstraat, Netherlands), directly inserted into the soft sediment. Below 10 m depth, we removed the more compact sediment samples from their liner and scraped off all potentially contaminated rims with a sterile scalpel. The remaining sediment was transferred into an IODP-style titanium pore water extraction cylinder (Mannheim et al., 1966) and placed on a 2-column bench top laboratory hydraulic press (Carver Inc., Wabash, USA). Pore water from both shallow and deep sediments was filtered through a sterile 0.2 μm syringe 30 filter and collected in a glass syringe pre-flushed with nitrogen. For anion analysis, 1 mL of pore water was transferred to a screw neck glass vial (VWR International, USA) and stored at 4°C until analysis.

Dissolved ferrous and ferric iron concentrations were measured in the field via spectrophotometry (Stookey, 1970). Directly after pore water retrieval, we aliquoted 1 mL of pore water sample to 1.6 mL Rotilabo single-use cells (Carl Roth, Karlsruhe, Germany) and stabilized dissolved Fe^{2+} by adding 100 μL of Ferrozine Iron Reagent (Sigma-Aldrich Chemie Munich, Germany). Absorbance of the colored solution was measured at 562 nm with a DR 3900 spectrophotometer (Hach, 5 Düsseldorf, Germany). To determine pore water total Fe concentrations, 150 μL of hydroxylamine hydrochloride were added to 800 μL of the previous mixture, left to react 10 min to reduce all dissolved Fe^{3+} , stabilized by adding 50 μL ammonium acetate and absorbance of the solution measured a second time (Viollier et al., 2000). Pore water total Fe concentrations were found to be the same as Fe^{2+} concentrations, and thus Fe^{3+} is absent in pore water. Detection limit of the method is 0.25 μM . Concentrations of PO_4^{3-} in pore water were measured by spectrophotometry. We aliquoted 0.5 mL pore water to 1.5 mL 10 disposable cuvettes (Brand GmbH, Germany) and added 80 μL color reagent consisting of ammonium molybdate containing ascorbic acid and antimony (Murphy and Riley, 1962). Absorbance was measured at 882 nm with a DR 3900 spectrophotometer (Hach, Düsseldorf, Germany). Detection limit of the method is 0.05 μM . Mn^{2+} concentrations were analyzed spectrophotometrically as previously published (Jones et al., 2011 and 2015), following the formaldoxime method (Brewer and Spencer, 1971). Pore water Ca^{2+} , Mg^{2+} and SO_4^{2-} concentrations were analyzed by normal and suppressed ion 15 chromatography as previously described (Vuillemin et al., 2016). Based on a respective signal-to-noise ratio of 3 and 10, detection and quantification limits of the method calibrated on a multi-element standard are 8.3 and 38.5 μM for Ca^{2+} , 9.6 and 44.6 μM for Mg^{2+} , and 2.0 and 8.4 μM for SO_4^{2-} . All samples were measured in triplicates, with reproducibility better than 5 %.

The pH was measured with a portable pH meter (Thermo Scientific Orion, Star A321) calibrated at pH 4, 7 and 10, 20 respectively. We homogenized 2 mL of sediment in 2 mL of deionized water and measured the supernatant after 2 min, which is the method commonly used to measure pH in organic-rich soil samples. We followed the published method no. 9045B from Black (1973) and calibrated our results based on the Standard Reference Material Catalog (Seward, 1986). Total alkalinity was measured via colorimetric titration on samples of Rhizon extracted and hydraulically squeezed pore water. Dissolved inorganic carbon (DIC) concentrations were calculated by solving the carbonate system using the pH and 25 alkalinity profiles and borehole temperatures (Jenkins and Moore, 1977). The complete pore water dataset, inclusive of all major cations and anions (Vuillemin et al., 2019a), was used to calculate mineral saturation indices based on pH, alkalinity, pore water concentrations and borehole temperatures, using the PHREEQC v.3 software (Parkhurst and Appelo, 2013).

2.4 Vivianite identification and crystal separation

The drill cores from TDP-1A remaining after field sampling of whole core rounds were split at LacCore, University of 30 Minnesota, USA. Split core halves were imaged at a resolution of 10 pixels/mm (~254 dpi) using a Geotek Geoscan-III with line-scan CCD cameras with fluorescent lights and polarizing filters to reveal core stratigraphy (Russell et al., 2016). Macroscopically visible vivianite crystals were hand-picked from split TDP-1A cores from 5 distinct horizons located

between 20 and 50 m sediment depth. Additional mineral separates of vivianite were obtained from core catchers. We mixed 50 mL of sediment with deionized water in a beaker and sonicated the slurry to homogenize and break up clay aggregates. The slurry was then separated with an initial settling time of ~2 min and removal of the supernatant. We separated the magnetic from the non-magnetic fraction in the settled dense fraction by placing a neodymium magnet below the beaker and 5 rinsing out the non-magnetic mineral fraction with deionized water, followed by drying with acetone. Minerals observed under a stereo microscope (Nikon SMZ800) included siderite, vivianite, millerite (i.e. NiS) and detrital pyroxene (i.e. Ca(Mg, Fe)Si₂O₆). Pyrite (i.e. FeS₂) was not observed. **Vivianite crystals, which were identified in the interval from 20 to 50 m sediment depth, were hand-picked under the stereo microscope for further analyses.**

2.5 X-ray powder diffraction

10 X-ray diffraction (XRD) patterns were obtained for one concentrated extract of powdered vivianite as well as for 6 samples of freeze-dried bulk sediment from different depths (i.e. 6.3, 12.4, 23.4, 52.7, 66.5, and 82.6 m), using a PANalytical Empyrean X-ray diffractometer (Eindhoven, The Netherlands), operating with a theta-theta goniometer at 40 kV and 40 mA and a PIXcel 3D detector. CuK α radiation was used with a step size from 4.6 to 85° 2 Θ and a count time of 1 min per step. The software packages AXS DIFFRACplus EVA and AXS Topas v. 4.2 (both Bruker) were used to identify minerals and 15 select peak references from the mineralogical database.

2.6 Field emission scanning electron microscopy

Isolated crystals of vivianite were mounted on 12.7 mm-diameter aluminum stubs with double-sided conductive carbon tape. An entire vivianite crystal was also embedded in epoxy and the stub cut in axial section. An ultra-thin coating of carbon was deposited on the samples by high-vacuum sputter coating using a Leica MED 020 BAL-TEC metallizer. Imaging was carried 20 out using an Ultra 55 Plus Schottky-type field emission scanning electron microscope. This microscope is equipped with an X-ray energy-dispersive (EDX) system and a Thermo Fisher Scientific silicon-drift detector (SDD UltraDry) for elemental analysis. Operating parameters were set at an acceleration voltage of 20 kV, working distance of 12.5 mm for secondary electron and back-scattering electron images, a 120 mm wide aperture, a silicon-drift detector take-off angle of 35°, and acquisition time of 30 s at a reduced count rate and dead time as needed for point analyses. Calculation of particle chemistry 25 was performed by applying the procedure of the Noran System Seven software based on the standardless matrix correction methods ZAF (i.e. atomic number, absorption, fluorescence) and $\phi(\rho z)$. Quantitative analyses of all detectable elements were normalized to 100 % atomic weight displayed as oxides. The detection limit for EDX ranges between 0.1 and 1 wt %.

2.7 Transmission electron microscopy

Preparation of electron-transparent vivianite samples was done with a FEI FIB200TEM focused ion beam (FIB) device. A 30 TEM-ready foil with final dimensions of 15 × 10 × 0.1 μ m was cut directly from the carbon-coated polished section using a

gallium ion beam under high-vacuum conditions and placed on a carbon film on top of a copper grid. Carbon-coating to prevent charging of the TEM sample was not applied (Wirth, 2009). The FIB-cut TEM foil was surveyed and analyzed using a FEI Tecnai G² F20 X-Twin transmission electron microscope. The microscope is equipped with an EDAX ultra-thin window EDX system, a Fishione high-angle annular dark-field (HAADF) detector, and a Gatan imaging filter. Operating conditions were set to an acceleration voltage of 200 kV, using normal imaging mode for bright-field and dark-field imaging and scanning transmission electron microscopy mode for HAADF imaging and analytical electron microscopy. All HAADF images were acquired with a camera length of either 75 or 330 mm. The short camera length (75 mm) allows to image Z contrast, whereas the long camera length (330 mm) allows simultaneous imaging of Z contrast and diffraction contrast. Bright-field images were digitally recorded. Semi-quantitative compositional spectra on both crystalline and amorphous phases were obtained from EDX spectrometer within 60-120 s live time. Beam size in scanning transmission electron mode was 1 to 2 nm and applied across the preselected areas during data acquisition. Structural information on crystalline phases was obtained from selected area electron diffraction patterns recorded on image plates for high precision.

2.8 Fe isotope analysis

After density separation, vivianite crystals were hand-picked under the stereo microscope and the isolated crystals processed for Fe isotope analyses at the HELGES lab, GFZ Potsdam (von Blanckenburg et al., 2016); however, the presence of some minor inclusions of siderite, silicates and oxides within vivianite crystals could not be ruled out. To avoid dissolution of silicates and oxides, about 5 mg of sample powder was leached with 2M HNO₃ for 24 hours at room temperature (von Blanckenburg et al., 2008). Complete dissolution of vivianite and a few solid residual particles were observed. After centrifugation, supernatants (dissolved vivianite and trace siderite) were evaporated in PFA vials on a hot plate at 110°C, then heated in closed vials at 150 °C with H₂O₂/HNO₃ and aqua regia to remove all OM. Procedure blanks and reference materials (USGS COQ-1 carbonatite rock, BHVO-2 basalt rock, HanFe pure Fe solution) were processed along with samples for quality control. After evaporation, samples were re-dissolved in 6M HCl and an aliquot of ~100 µg Fe was passed through chromatographic columns (DOWEX AG-X8 resin) to purify Fe from other matrix elements (Schoenberg and von Blanckenburg, 2005). Purity and quantitative recovery of Fe was verified by inductively coupled plasma - optical emission spectrometry (ICP-OES, Varian 720ES) and found to be better than 98 %. Cr and Ni were efficiently separated from Fe, thus eliminating spectral interferences of ⁵⁴Cr on ⁵⁴Fe and ⁵⁸Ni on ⁵⁸Fe. Blanks of all procedures were measured by quadrupole ICP-MS (Thermo iCAP-Qc) and contained <10 ng Fe, thus contributing to <0.01 % of processed Fe samples (~100 µg), and are therefore considered negligible.

Prior to isotope analysis, samples were dissolved in 0.3 M HNO₃ and diluted to ~5 µg mL⁻¹ Fe to match the concentration of the bracketing standard (IRMM-014) within 10 %. Fe isotopic analyses were performed using a Thermo Scientific Neptune multi-collector inductively coupled plasma mass spectrometer (MC-ICP-MS) equipped with a Neptune Plus Jet Interface pump and a quartz-glass spray chamber (double pass cyclon-scott type, Thermo SIS) with a 100 µL min⁻¹ self-aspirating PFA nebulizer for sample introduction. Analyses were run in high mass resolution mode (mass resolving power m/Δm (5 %,

95 %) ~9000) to resolve all Fe isotopes from polyatomic interferences (i.e. ArO, ArOH, and ArN). Potential interferences of ^{54}Cr on ^{54}Fe and ^{58}Ni on ^{58}Fe were monitored at masses ^{52}Cr and ^{60}Ni . The sample-standard bracketing method (using IRMM-014 as bracketing standard) was used to correct for instrumental mass bias (Schoenberg and von Blanckenburg, 2005). Isotope ratios ($^{56}\text{Fe}/^{54}\text{Fe}$ and $^{57}\text{Fe}/^{54}\text{Fe}$) are reported in the δ -notation in per mil (‰) relative to the international reference material IRMM-014 (e.g., $\delta^{56}\text{Fe} = (^{56}\text{Fe}/^{54}\text{Fe}_{\text{sample}}/^{56}\text{Fe}/^{54}\text{Fe}_{\text{IRMM-04}} - 1) \times 1000$). Measurements were repeated between 2 and 8 times in two independent analytical sessions. Results of $\delta^{57}\text{Fe}$ and $\delta^{56}\text{Fe}$ all follow mass-dependent isotope fractionation and therefore results are only discussed in terms of $\delta^{56}\text{Fe}$ with an uncertainty of the method estimated to be $\pm 0.05\text{ ‰}$ (2σ) in $\delta^{56}\text{Fe}$, as verified during this study by repeated analyses of reference materials and comparison to published reference values (Supplementary Table S1).

10 3 Results

3.1 Lithology and core scanning images

The lithology of TDP site 1 is displayed from 0 to 100 m depth (Fig. 2a), ending at the boundary between the predominantly fine-grained lacustrine Unit 1 and the more coarse-grained fluvio-lacustrine Unit 2 (Russell et al., 2016). The upper 100 m of sediment consist largely of alternating dark reddish-grey and brown to dark-green grey lacustrine clay beds (Fig. 2a-b).
15 Turbidites are relatively rare but more common below 50 m and above 25 m depth and two ~5 m beds of diatom ooze occur at ~35 and 45 m depth. We also observed tephras throughout Unit 1. We focus on 5 intervals containing vivianites between 20 and 50 m depth, where sediment types include both red and green clays, diatomaceous oozes and several large tephras (Fig. 2a). Vivianites are mostly found in green clays, often overlain by siderite-rich red clays and, occasionally, turbidites (Supplementary Fig. S3). Diatomaceous oozes are devoid of vivianite and siderite. A more detailed description of the full 20 stratigraphy is published elsewhere (Russell et al., 2016).

3.2 Total organic carbon, reactive and total iron

Over the upper 100 m of the sediment sequence at site TDP-1A, TOC values (Fig. 2a) vary between ~6 and 0.2 wt %. The upper 20 m of sediments display concentrations fluctuating between 3.5 and 0.5 wt % with an overall decrease with depth. In the vivianite-bearing interval (20-50 m), values reach maxima of ~3 wt % in the diatomaceous oozes. In the lowermost part 25 of the record, TOC gradually increases from 1.0 wt % at 50 m depth to 4.0 wt % at 80 m depth, with highest values (~6%) at the bottom of the core just above the peat layer.

Reactive Fe concentrations vary from 7 to 12 wt % within the upper 20 m of the sediment record, fluctuate between 5 and 15 wt % with the vivianite-bearing interval, and remain relatively constant around 15 wt % below. Total Fe concentrations generally fluctuate between 15 and 20 wt % in Unit 1, with the exception of the interval between 50 and 80 m depth where

values occasionally reach 25 to 30 wt %. Some of these high values occur within turbidite beds. The lowest values (~7 wt %) are found within the diatomaceous oozes at 35 and 45 m depth, and just above a peat layer at ~100 m depth.

3.3 Pore water geochemistry and modeled saturation indices

In the upper 20 m of sediment, pore water DIC concentrations increase gradually from 2 to 6 mM with depth. Values drop to 4 mM at 20 m depth and then increase gradually from 4 to 7 mM down to 100 m depth. Profiles for pore water Ca^{2+} and Mg^{2+} concentrations display similar trends, with maximum values observed within the upper 15 m of sediment followed by a drop of their respective values from 200 and 600 μM to close to zero. Pore water PO_4^{3-} concentrations in the upper 10 m of sediments increase gradually from 0 to 0.62 μM with depth. Between 20 and 50 m depth, values remain low (0.15 to 0.20 μM). Concentrations of pore water Mn^{2+} are initially ~5 μM in the upper meter of the sediment, minimal in the next 10 m of 10 sediment, and then increase to 20 μM down to 20 m depth. With the vivianite bearing-interval, Mn^{2+} concentrations gradually decrease to a minimum at 50 m depth. Concentrations of pore water SO_4^{2-} were often close to our quantification limit (8.4 μM), with concentrations between 10 and 25 μM . Slightly increased concentrations are observed around 75 m depth. Concentrations of pore water Fe^{2+} are highly variable throughout the sedimentary sequence (17-278 μM). Some of the intervals with highest dissolved Fe^{2+} values are found in the uppermost part of the record (1-6 m), from 15-20 m depth just 15 above the vivianite interval, and in the lowermost section of the core (90-100 m). Below 50 m depth, both Fe^{2+} and PO_4^{3-} values generally peak in the vicinity of turbidite layers.

Geochemical modeling of the pore water chemistry indicates supersaturation with respect to siderite at 5 m depth (1.29) and over the entire lower sediment sequence (Table 1). In contrast, vivianite is undersaturated in pore water at 5 m (-0.45) and reaches close to, but remains below saturation (-0.04) in sediment at 10 m depth. Talc/serpentine is supersaturated in shallow 20 sediment and becomes undersaturated with depth, whereas quartz is stable under in situ conditions. XRD spectra further support the presence and stability of specific phases, such as siderite, quartz, and serpentine (Supplementary Fig. S2).

3.4 Iron isotopes

Iron isotopes measured on single vivianite crystals (Fig. 2a) display $\delta^{56}\text{Fe}$ values of -0.52 ‰ and -0.44 ‰ at 23 m depth, -0.61 ‰ at 36 m depth, and -0.39 ‰ and -0.46 ‰ at 46 m depth (all ± 0.05 ‰, 2 σ). We observe the most negative 25 $\delta^{56}\text{Fe}$ values in a specimen from the middle of the vivianite-bearing interval. The iron incorporated in the measured vivianite crystals is isotopically lighter in comparison to the global bulk igneous rock reservoir ($\delta^{56}\text{Fe} = +0.1 \pm 0.1$ ‰, e.g. Dauphas et al., 2017 and references therein), which is the value expected for the ultramafic igneous rocks in Lake Towuti's catchment. To the best of our knowledge, there are no existing data on vivianite $\delta^{56}\text{Fe}$ in the literature that would allow comparison. As 30 such, Fe isotope fractionation factors remain unknown for vivianite formation. However, previous studies indicate that during Fe redox reactions, the Fe^{2+} -bearing phases generally become enriched in the lighter Fe isotopes compared to Fe^{3+} -bearing phases (e.g., Dauphas et al. 2017). Given that vivianite is a Fe^{2+} -bearing mineral phase, the isotopically light $\delta^{56}\text{Fe}$

values we measured in vivianites from Lake Towuti are consistent with the direction of fractionation occurring during Fe³⁺ reduction. However, dissolution of precursory ferrous phases could also be the source of the Fe²⁺ incorporated in vivianite crystals.

3.5 Vivianite detection, SEM imaging, EDX analysis

5 The XRD pattern of our powdered vivianite extract confirms identification of this mineral, with an excellent match to reference peaks of one synthetic vivianite from the mineral database (Fig. 3c). Larger vivianite concretions were not observed upon inspection of split core surfaces. Vivianite was also not detected in XRD patterns of bulk sediment at 6 different depths. Siderite, quartz (i.e. SiO₂) and serpentine (i.e. lizardite: Mg₃Si₂O₅(OH)₄) were the main minerals clearly identified based on reference peaks in these 6 samples, whereas vivianite was below the XRD detection limit of 1 %
10 (Supplementary Fig. S2).

SEM images of single vivianite crystals (Fig. 3a) show that the habit varies from tabular crystals at 23 m depth to rosette at 36 m depth with addition of blades and overall growth at 46 m depth, and the largest crystal (>7 cm) being found at 50 m depth. EDX points of analysis indicate partial substitution of Fe²⁺ by Mn²⁺ in the structure of vivianite crystals from 23 and 36 m depth (up to ~17% Fe substitution), resulting in their overall “manganoan” composition (Fig. 3b). Such compositions
15 have been previously reported from both freshwater and marine sediments although with variable Mn concentrations (Fagel et al., 2005; Dijkstra et al., 2016). High Fe content outside the stoichiometric range of vivianite indicates the presence of residual oxides within the crystals. SEM images with location of all EDX points of analysis are available as supplement (Supplementary Fig. S4).

3.6 EDX elemental mapping, TEM imaging

20 SEM images of the vivianite thin section in back-scattering electron mode reveal a central tabular crystal and imply growth of subsequent blades with preferential orientation directed towards the sediment surface (Fig. 4a). Close-ups also reveal the presence of mineral inclusions entrapped within the central tabular blade and upper side of the vivianite (Fig. 4a), namely siderite (1), millerite (2) and goethite (3). Siderite appears in the form of aggregated nanocrystals, millerite in a micro-acicular habit forming radiating aggregates, and goethite in irregular sheets whose jagged edges and dissolution features
25 likely indicate a detrital origin and potentially partial sedimentary dissolution from iron reduction. EDX elemental mapping (Fig. 4b) as well as individual analyses (Fig. 4c) confirms the composition and identity of these inclusions. Increased intensities of Fe and Mn correspond to goethite, S and Ni to millerite, while those of Si and Al indicate the presence of phyllosilicates inside and between vivianite blades. Ternary diagrams for individual EDX analyses show that millerite incorporates traces of iron, whereas traces of Mn in iron oxides indicates goethite rather than hematite in which Fe
30 substitution by Mn is limited (Singh et al., 2000).

Scanning TEM imaging of Z contrast and diffraction contrast (i.e. 330 nm) show that the vivianite sample from 46.8 m depth has a denser structure than the one from 36.7 m depth. Close-up images reveal the presence of iron oxides (a), illite

clays (b) and detrital pyroxene (c), as confirmed by their EDX analyses, which show that vivianite incorporates phases of detrital origin. Fractures in the crystal from 36.7 m depth could be due to its partial oxidation and dehydration (Hanzel et al., 1990), or to immaturity relative to the sample from 46.8 m depth. Finally, the high resolution electron diffraction pattern of the deepest (oldest) vivianite sample from 46.8 m depth demonstrates its well-ordered monoclinic structure (d), whereas the 5 pattern of the one from 36.7 m depth is somewhat kinked.

4 Discussion

4.1 Early microbial diagenesis and vivianite growth

In aquatic systems and surface sediments, Fe chemistry influences the distribution of dissolved sulfide, the solubility of trace metals, and bioavailability of P and thereby controls their rates of burial (Severmann et al., 2006). The formation of vivianite

10 in sediments often results from small-scale microbially mediated reactions (Rothe et al., 2016), such as reduction of ferric Fe minerals, with partial dissolution and/or precipitation of mineral phases (Rothe et al., 2014; Egger et al., 2015; Tamuntuan et al., 2015; Dijkstra et al., 2016), alongside OM decomposition (Gächter et al., 2003; Hupfer and Lewandowski, 2008). In Fe-rich, SO_4^{2-} -poor, oligotrophic settings like Lake Towuti and Lake Matano where HS^- production is minimal (Vuillemin et al., 2016), the first authigenic Fe minerals expected to form via the reduction of ferrihydrite are mixed-valence iron oxides (e.g. 15 green rust, magnetite) instead of sulfides (Crowe et al., 2008; Zegeye et al., 2012; Vuillemin et al., 2019a). In nearby Lake Matano, lake waters contain more than 40 nM Ni and are supersaturated with respect to millerite where sulfide accumulates to low μM concentrations (Crowe et al., 2008). By analogy to Lake Matano, Ni would compete with Fe for sulfide in Lake Towuti and its sediments. Indeed, we observed the presence of diagenetic millerite in the sediment (Fig. 4) which forms due to the preferential reaction of HS^- with dissolved Ni^{2+} instead of Fe^{2+} (Ferris et al., 1987). Since SO_4^{2-} concentrations are 20 mostly below 50 μM in the core (Fig. 2a), potential rates of sulfide production remain very low compared to the Fe delivery flux and, because Ni is also abundant, HS^- production has a negligible effect on P release from the sediment. Such low SO_4^{2-} concentrations further result in the loss of most sulfate, and increased methanogenesis, within the first upper meter of sediment (Vuillemin et al., 2018). As a result, processes of OM remineralization are predominantly driven by fermentation 25 and methanogenesis (Friese et al., 2018) and DIC steadily increases with depth (Fig. 2a). Thus, in sediments such as Lake Towuti's, siderite is an expected mineral phase, and indeed siderite is abundant in some of Towuti's sediments (Ordoñez et al., 2019; Vuillemin et al., 2019a). This implies that CO_3^{2-} can compete with PO_4^{3-} for available Fe^{2+} . Modeled mineral saturation indices confirmed this, as pore waters are saturated with respect to siderite at 5 m sediment depth and below. In comparison, vivianite remains close to, but slightly below saturation in deep sediments (Table 1).

We observed an apparent progression in vivianite morphology from tabular to rosette with increasing depth down core (Figs. 30 3a and Supplementary Fig. S4). Vivianite crystals develop radially and vertically during diagenesis, incorporating authigenic phases and detrital silicates within the crystal and between blades (Figs. 4-5, and Supplementary Fig. S5). Authigenic phases (e.g. siderite, millerite) and detrital oxides (e.g. goethite) were trapped within these crystals (Fig. 4a). Millerite is mainly

observed in the tabular template, whereas siderite and goethite are found in the upper blades of the crystal (Figs. 4a-4b). The fact that authigenic siderite and millerite are observed within vivianite crystals demonstrates that vivianite forms at a later stage of diagenesis. Vivianite crystals display growth orientation toward the sediment surface, as shown by the development of successive rosettes on site (Supplementary Fig. S5). In pelagic fine sediments, crystals build up to form successive 5 spherules stacked on top of each other reaching sizes of ~4 to 7 cm (Supplementary Figs. S3 and S5).

Concentrations of Fe oxides in Lake Towuti's sediment are high (~ 20 wt %), and iron oxides such as goethite persist in the modern sediment even under full anoxia at the water-sediment interface and below (Sheppard et al., 2019). If PO_4^{3-} could diffuse out of the sediment, the whole-lake Fe, P and oxygen dynamics predict that any P that might escape to the photic zone from deep, anoxic settings can be buried in shallow-water, oxidized sediments. In the deep sediments, pore water PO_4^{3-} 10 concentrations are constantly low in the interval where vivianite crystals are observed (Fig. 2a), suggesting that vivianites could act as a P sink from the pore water to the sediment during diagenesis (Vuillemin et al., 2013, 2014). Dissolved Fe^{2+} concentrations are not particularly low and fluctuate (40-100 μM), suggesting excess Fe relative to P and potentially reflecting dissolution of detrital phases (e.g. ferrihydrite, goethite, hematite) and/or precipitation of authigenic ones (e.g. magnetite, siderite, vivianite). In contrast, Fe^{3+} concentrations in pore water are already depleted in the upper meter of 15 sediment, whereas concentrations of DIC, which is produced during OM degradation, gradually increase with depth (Fig. 2a), suggesting that OM remineralization in shallow sediment is mainly driven by fermentation and methanogenesis rather than microbial Fe reduction (Vuillemin et al., 2018). In the vivianite-bearing intervals, DIC concentrations remain rather constant (4 mM). An explanation for this is that, once pore water Fe^{3+} and SO_4^{2-} concentrations are depleted as a result of microbial reduction within the first meter of sediment, OM remineralization mostly occurs by CO_2 reduction and 20 methanogenesis (Friese et al., 2018). The onset of autotrophic methanogenesis is expected to reduce DIC activity in pore water and to draw down PO_4^{3-} cycling by microbes. Moreover, Ca^{2+} and Mg^{2+} concentrations in pore water, which are predicted to control the solubility of PO_4^{3-} in ferruginous systems (Jones et al., 2015), drop around these depths as divalent cations can precipitate during siderite formation (Vuillemin et al., 2019a), suggesting that PO_4^{3-} can then outcompete CO_3^{2-} for available Fe^{2+} and thereby saturate pore water with respect to vivianite (Table 1). Vivianite formation is indeed reported 25 to occur under methanogenic conditions, often initiating below the sulfate-methane transition zone (Reed et al., 2011; Dijkstra et al., 2016), presently located within the upper meter of sediment (Vuillemin et al., 2018). Inclusions of millerite and siderite within vivianite crystals (Fig. 4) provide additional lines of evidence for microbial processes of pore Fe^{3+} and SO_4^{2-} reduction and DIC production prior to vivianite formation. The saturation indices modeled for vivianite (Table 1) and 30 downcore profiles of Mn^{2+} and PO_4^{3-} concentrations allow to infer a depth in the sediment at which pore waters initially reached saturation with respect to vivianite (ca. 20 m depth). Such relationship between dissolved Mn^{2+} and PO_4^{3-} is also consistent with EDX punctual analyses of vivianite crystals that show Mn^{2+} incorporation at an early stage (Fig. 3b, Supplementary Fig. S4).

However, the fact that dissolved PO_4^{3-} , Mn^{2+} , Fe^{2+} and DIC vary independently also implies a decoupling in their production and consumption rates (e.g. through mineral formation and microbial metabolic consumption), such that they are not simply linked through steady-state OM respiration coupled to Fe reduction.

4.2 Past lacustrine conditions promoting vivianite formation during burial

5 In sulfur-poor, ferruginous settings, vivianite, siderite and magnetite can be formed in the sediments (Postma, 1981) depending on the local pH, CO_2 , PO_4^{3-} , the amount and reactivity of ferric oxides and OM buried in the sediment (Fredrickson et al., 1998; Glasauer et al., 2003; O'Loughlin et al., 2013). By analogy to hydromorphic soils (Maher et al., 2003; Vodyanitskii and Shoba, 2015), redox conditions at the time of deposition and fluxes of OM and reactive ferric oxides to the sediment would select for siderite or vivianite as the main diagenetic ferrous end-members during burial. In shallow 10 sediment cores spanning the last ~60 kyr, Costa et al. (2015) suggested that elevated Fe concentrations represent time intervals of enhanced lake mixing. The alternating dark reddish-brown and lighter green/grey beds, in which vivianites were found in the deeper TDP cores (Fig. 2b, Supplementary Fig. S3), also suggest variable oxygenation at the water-sediment interface in the past (Costa et al., 2015; Russell et al., 2016). Some vivianite-bearing beds appear at similar locations in multiple holes, suggesting lake-wide chemical conditions promoted diagenetic growth of vivianite in the sediment during 15 later burial (Supplementary Fig. S4). However, in other cases, vivianites appear sporadically in only one core. Below the layer in which the biggest vivianite crystal (>7 cm) was found (~50 m sediment depth), we observe increased iron concentrations (>30 %) corresponding to siderite-rich sediments and multiple turbidites (~50 to 60 m; Fig. 2a). Sporadic turbidites could result in discrete layers enriched in siderites, which are sometimes also linked to bottom water oxygenation, due to enhanced deposition of iron oxides and precipitation of HCO_3^- and Fe^{2+} shortly after deposition (Hasberg et al., 2019; 20 Sheppard et al., 2019). Such turbidites may also promote sporadic laterally non-contiguous vivianite formation in one site (Supplementary Fig. S4). For instance, a large flat-topped vivianite crystal (>4 cm) capped by a turbidite shows how rapid sedimentary processes prevent further growth of this mineral (Supplementary Fig. S5). Within the vivianite-bearing interval (20-50 m depth), diatomaceous oozes signify relatively high primary productivity, and 25 their corresponding iron concentrations are lowest, which is consistent with the absence of siderite and vivianite therein (Fig. 2a). Below and above this interval, vivianites are rarely present in the sediment, which was confirmed by smear slide analysis (Russell et al., 2016), and X-ray diffraction (Supplementary Fig. S2). The substantial fossilization of diatoms, with vivianites below and above these sediments, could reflect higher P concentrations in the water column during this time interval compared to present-day levels, pointing either to increased P supply to the basin and/or a change in P recycling. Given the slow sedimentation rates (~0.2 m kyr^{-1}) in the upper 10 m of sediments (Russell et al., 2014), it seems likely that 30 the 20-50 m interval encompasses at least 100 kyr. During the Last Glacial Maximum (LGM), Towuti's lake level was 15 to 30 m lower than today, possibly resulting in endorheic conditions (Costa et al., 2015; Vogel et al., 2015). By analogy, lake levels may have been lower during preceding glacial phases, at least one of which is likely to be included in the vivianite-bearing interval. While lake shrinkage could affect algal productivity in the remaining waters (Clavero et al., 1993; Schütt,

1998; Bernal-Brooks et al., 2003; Recasens et al., 2015), lower lake levels should promote bottom water oxygenation and burial of Fe-oxides, and thereby suppress P recycling. Tephras, if they bear apatite (i.e. $\text{Ca}_5(\text{PO}_4)_3(\text{OH})$) or additional P adsorbed onto their mineral phases, could represent an additional source of P to the lake (Harper et al., 1986; Nanzyo et al., 1997; Ayris and Delmelle, 2012). As P concentrations tend to affect algal phytoplankton productivity as a whole (Zhang and Prepas, 1996; Van der Grinten et al., 2004), high Si concentrations in the lake represent an additional factor promoting the preservation of diatoms over cyanobacteria during sinking and burial. Finally, sediment-starved conditions would also limit P scavenging in the water column. In contrast, increased delivery of detrital iron (oxyhydr)oxides precipitates P to the sediment and initially forms sideritic beds, whereas vivianite formation initiates under slow kinetics deeper in the sediment than for siderite (Postma, 1981) as demonstrated by the incorporation of siderite, millerite and clay minerals in the vivianites (Figs. 4 and 5).

4.3 $\delta^{56}\text{Fe}$ compositions of vivianites and implications for the Archean rock record

Previous Fe isotope studies of lakes identified either partial oxidation of Fe^{2+} in the water column or microbial iron reduction below the sediment-water interface as the main drivers for Fe pathways and isotope fractionation (Teutsch et al., 2009; Song et al., 2011; Liu et al., 2015). Depending on rates of reduction and dissolution (Brantley et al., 2001), dissimilatory microbial reduction of iron releases Fe^{2+} that is up to 2 ‰ lighter than the original substrates (Crosby et al., 2007; Tangalos et al., 2010), therefore iron isotopes are commonly used to trace redox processes related to microbial activity in aquatic sediments (Percak-Dennett et al., 2013; Busigny et al., 2014). During sediment early diagenesis, the preferential dissolution of isotopically light Fe^{2+} leaves behind an increasingly heavier residual Fe pool (Staubwasser et al., 2006), which results in the diffusive accumulation of the light isotopes in the top layer of sediments where they can be adsorbed and incorporated into ferrous Fe phases. The $\delta^{56}\text{Fe}$ values reported for pore water Fe^{2+} in lacustrine sediments range between -2 and -1 ‰ and become heavier with depth as authigenic phases form (Song et al. 2011; Percak-Denett et al. 2013). The $\delta^{56}\text{Fe}$ values for reduced Fe phases formed in the sediment are highly variable and range from -1.5 to -0.8 ‰ for pyrite (Busigny et al., 2014), -1.6 to 0.3 ‰ for siderite (Johnson et al., 2005) and -0.1 to 0.2 ‰ for magnetite (Percak-Denett et al. 2013).

Compared to the global bulk igneous rock reservoir ($\delta^{56}\text{Fe} = +0.1 \pm 0.1 \text{ ‰}$) and ultramafic rocks (Dauphas et al. 2017) such as those present in Lake Towuti's catchment, the $\delta^{56}\text{Fe}$ measured on whole vivianite crystals (-0.61 to -0.39 ‰) reveals incorporation of isotopically fractionated light Fe^{2+} (Fig. 2a), even though traces of detrital iron-bearing minerals and secondary oxides are present within vivianite crystals (Figs 4 and 5). Towuti's Fe mineralogy from source to sink reflects complex cycling of Fe as iron minerals derived from catchment soils (e.g. goethite, hematite, magnetite) tend to transform into nanocrystalline Fe phases during reductive dissolution in the lake water column and sediment (Tamuntuan et al., 2015; Sheppard et al., 2019). Ferric/ferrous phases precipitating in equilibrium at the oxycline or during mixing events could be abiotically fractionated to 1-2 ‰ heavier/lighter isotope values than the remaining aqueous Fe^{2+} (Bullen et al., 2001; Skulan et al., 2002; Beard et al., 2010; Wu et al., 2011). After deposition, partitioning of the light Fe isotopes mainly transits

through release to pore water (Henkel et al., 2016) implying a succession of mineral transformation and dissolution with internal diagenetic Fe redistribution during burial (Severmann et al., 2006; Scholz et al., 2014). For instance, mixed-valence iron oxides (e.g. green rust), which are authigenic phases that form initially under ferruginous conditions (Zegeye et al., 2012; Vuillemin et al., 2019a) are highly sorbent for pore water HCO_3^- and HPO_4^{2-} and can thereby transform into either 5 siderite or vivianite as the sediment ages (Hansen and Poulsen, 1999; Bocher et al., 2004; Refait et al., 2007; Halevy et al., 2017). Because vivianite formation initiates in the sediment, we infer that vivianite crystals acted as additional traps for the reduced Fe^{2+} released to pore water and that their light $\delta^{56}\text{Fe}$ values are consistent with kinetic fractionation related to microbial Fe reduction during early diagenesis, or eventually inherited from post-depositional dissolution of transient ferrous 10 phases. In the latter case, pre-depositional processes of abiotic Fe fractionation related to stratified conditions will require further investigations.

Whether they relate to microbial reduction in soft ferruginous sediment or past conditions in bottom waters, biotic and abiotic diagenetic processes remain challenging to constrain in terms of ancient rock record (Johnson et al., 2013). Concentrations estimates for deep anoxic waters interpreted from the Archean rock record typically range from 40 to 120 15 μM for Fe and 0.1 to 0.3 μM for P (Holland, 2006; Konhauser et al., 2007; Jones et al., 2015), which are similar to those presently observed in the pore water of ferruginous analogue Lake Towuti (Fig. 2a). Concerning P diagenesis, it is hypothesized that P availability in the Archean ocean was limited by the lack of terminal electron acceptors and oxidative power used to recycle most of the OM-bound P rather than by scavenging by Fe minerals (Kipp and Stüeken, 2017; Michiels et al., 2017; Herschy et al., 2018). The present Ca^{2+} and Mg^{2+} concentrations in pore water exert apparent control on the 20 precipitation of siderite and/or vivianite during early diagenesis (Vuillemin et al., 2019a), which is comparable to interpretations of ancient P availability in regards to hydrothermal and continental weathering of mafic rocks (Jones et al., 2015). In this context because secondary P-bearing minerals cannot form if P remains bound to OM, we suggest that the precipitation of millerite, siderite, and vivianite in the sediment constitute a likely diagenetic sequence stemming from the depletion of pore water electron acceptors and related loss of oxidative power during OM remineralization, with consequent long-term P sequestration .

25 5. Conclusions

Non-steady state conditions likely promoted the sporadic formation of diagenetic vivianites within otherwise siderite-rich sediments during a prolonged interval of ferruginous Lake Towuti's history. Although the source of P is not well constrained, its inputs stimulated diatom productivity and sporadic vivianite formation during diagenesis. Inclusions of millerite, siderite and partially dissolved goethite within vivianite crystals support the assumption that microbial Fe^{3+} and 30 SO_4^{2-} reduction took place prior to vivianite formation. With depth and over time, vivianite crystals grew and changed from tabular to rosette morphologies, including surrounding clays. The corresponding $\delta^{56}\text{Fe}$ compositions confirmed that these crystals incorporated microbially fractionated light Fe^{2+} during diagenesis. While these light isotopic signatures may also

point to pre-depositional Fe fractionation related to lake stratification and dissolution of transient ferrous phases, the precipitation of millerite, siderite, and vivianite along burial in ferruginous sediment is consistent with the gradual depletion of pore water electron acceptors and related loss of oxidative power during OM remineralization, which results in long-term sequestration of P as vivianite. Thus, identification of these diagenetic phases could be used to interpret post-depositional processes of microbial reduction, and thereby help constrain early diagenesis timewise.

Data availability

Present scientific data are archived and publicly available at PANGAEA® Data Publisher for Earth & Environmental Science (Vuillemin et al., 2019b).

Author contributions

10 AV designed the study, sampled in the field, extracted vivianite crystals, actively took part in SEM, TEM, and XRD analyses, designed the figures and led the writing of the present manuscript. AF sampled in the field and measured pore water geochemistry. RW operated the TEM. JAS and FvB processed and measured iron isotopes. AMS led XRD analyses. HK led SEM analyses. AL led TOC analyses. KWB processed and measured samples for total iron and pore water iron. SN measured pH in the field. RS measured alkalinity in the field. LO sampled in the field and processed cores at LacCore. DA 15 processed and sampled cores at LacCore. CH fulfilled the research permit procedure. As principal investigators of the Towuti Drilling Project, JMR, SB, HV sampled in the field, processed drill core splitting and imaging at LacCore, processed TOC and Fe concentrations on full cores, and supervised the writing of the present manuscript. SAC sampled in the field, fulfilled the research permit procedure, supervised iron analyses and writing of the present manuscript. JK sampled in the field and at LacCore, supervised geochemical analyses and writing of the present manuscript. The Towuti Drilling Project 20 Science Team actively participated in drilling operations and processing of the cores at LacCore.

Competing interests

The authors declare that they have no conflict of interest.

Acknowledgements

This research was carried out with partial support from the International Continental Scientific Drilling Program (ICDP), the 25 U.S. National Science Foundation (NSF), the German Research Foundation (DFG), the Swiss National Science Foundation (SNSF), PT Vale Indonesia, the Ministry of Research, Education, and Higher Technology of Indonesia (RISTEK), Brown University, the University of Minnesota, the University of Geneva, GFZ German Research Centre for Geosciences, the

Natural Sciences and Engineering Research Council of Canada (NSERC), and Genome British Columbia. This study was financially and logically supported by the DFG ICDP priority program through grants to JK (KA 2293/8-1) and AV (VU 94/1-1), an SNSF grant to AV (P2GEP2_148621) and an NSERC Discovery grant (0487) to SAC.

We thank PT Vale Indonesia, the U.S. Continental Scientific Drilling and Coordination Office, and U.S. National Lacustrine 5 Core Repository, and DOSECC Exploration Services for logistical support. The research was carried out with permissions from RISTEK, the Ministry of Trade of the Republic of Indonesia, the Natural Resources Conservation Center (BKSDA), and the Government of Luwu Timur of Sulawesi. We thank the Director of the Indonesia Research Center for Limnology 10 (P2L) - Indonesian Institute of Sciences (LIPI), Tri Widiyanto and his staff of P2L-LIPI for their administrative support in obtaining the Scientific Research Permit. Supervision by the scientific crew of LacCore during core splitting and 15 subsampling is kindly acknowledged. We also thank Aan Diyanto, Axel J. Kitte, Anja Schreiber, Ilona Schäpan and Johannes Glodny for their assistance during field sampling, TEM and SEM analyses and mineral extractions, respectively.

Team members

Other members of the TDP Science Team are M. Melles, S. Fajar, A. Hafidz, D. Haffner, A. Hasberg, S. Ivory, C. Kelly, J. King, K. Kirana, M. Morlock, A. Noren, R. O'Grady, J. Stevenson, T. von Rintelen, I. Watkinson, N. Watrus, S. 15 Wicaksono, T. Wonik, A. Deino, A. M. Imran, R. Marwoto, L. O. Ngkoimani, L. O. Safiuddin, and G. Tamuntuan.

References

Ayris, P. M., and Delmelle, P.: The direct environmental effects of tephra emission, *Bull. Volcanol.*, 74, 1905-1936, <https://doi.org/10.1007/s00445-012-0654-5>, 2012.

20 Bauer, K. W., Byrne, J., Kenward, P., Simister, R., Michiels, C., Friese, A., Vuillemin, A., Henny, C., Nomosatryo, S., Kallmeyer, J., Kappler, A., Smit, M., Francois, R., Crowe, S. A.: Magnetite biomineralization in ferruginous waters and early Earth evolution, *EarthArXiv Preprint*, <https://doi.org/10.31223/osf.io/prhuz>, 2020.

Beard, B. L., Handler, R. M., Scherer, M. M., Wu, L., Czaja, A. D., Heimann, A., and Johnson, C. M.: Iron isotope fractionation between aqueous ferrous iron and goethite, *Earth Planet. Sc. Lett.*, 295, 241-250,

25 <https://doi.org/10.1016/j.epsl.2010.04.006>, 2010.

Bernal-Brooks, F. W., Dávalos-Lind, L., and Lind, O. T.: Seasonal and spatial variation in algal growth potential and growth-limiting nutrients in a shallow endorheic lake: Lake Pátzcuaro (Mexico), *Lakes Reserv. Res. Manag.* 8, 83-93, <https://doi.org/10.1046/j.1320-5331.2003.00217.x>, 2003.

Black, C. A. (Ed.): *Methods of Soil Analysis: Test Methods for Evaluating Solid Waste, Physical/Chemical Methods*, 9045B

30 *Soil and Waste pH*, American Society of Agronomy, Madison, USA, 1973.

Bocher, F., Géhin, A., Ruby, C., Ghanbaja, J., Abdelmoula, M., and Génin, J.-M. R.: Coprecipitation of Fe(II–III) hydroxycarbonate green rust stabilized by phosphate adsorption, *Solid State Science*, 6, 117–124, <https://doi.org/10.1016/j.solidstatesciences.2003.10.004>, 2004.

Bramburger, A. J., Hamilton, P. B., Hehanussa, P. E., and Haffner, G. D.: Processes regulating the community composition and relative abundance of taxa in the diatom communities of the Malili Lakes, Sulawesi Island, Indonesia, *Hydrobiologia*, 615, 215–224, <https://doi.org/10.1007/s10750-008-9562-2>, 2008.

Brantley, S. L., Liermann, L., and Bullen, T. D.: Fractionation of Fe isotopes by soil microbes and organic acids, *Geology*, 29, 535–538, [https://doi.org/10.1130/0091-7613\(2001\)029<0535:FOFIBS>2.0.CO;2](https://doi.org/10.1130/0091-7613(2001)029<0535:FOFIBS>2.0.CO;2), 2001.

Brewer, P. G., and Spencer, D. W.: Colorimetric determination of manganese in anoxic waters, *Limnol. Oceanogr.*, 16, 107–110, <https://doi.org/10.4319/lo.1971.16.10107>, 1971.

Bullen, T. D., White, A. F., Childs, C. W., Vivit, D. V., and Schulz M. S.: Demonstration of significant abiotic iron isotope fractionation in nature, *Geology*, 29, 699–702, [https://doi.org/10.1130/0091-7613\(2001\)029<0699:DOSAII>2.0.CO;2](https://doi.org/10.1130/0091-7613(2001)029<0699:DOSAII>2.0.CO;2), 2001.

Busigny, V., Planavsky, N. J., Jézéquel, D., Crowe, S., Louvat, P., Moureau, J., Viollier, E., and Lyons, T. W.: Iron isotopes in an Archean ocean analogue, *Geochim. Cosmochim. Ac.*, 133, 443–462, <https://doi.org/10.1016/j.gca.2014.03.004>, 2014.

Clavero, V., Garcia, M., Fernández, J. A., and Niell, F. X.: Adsorption-desorption of phosphate and its availability in the sediment of a saline lake (Fuente de Piedra, southern Spain), *Int. J. Salt Lake Res.* 2, 153–163, <https://doi.org/10.10007/BF02905907>, 1993.

Compton, J., Mallinson, D., Glenn, C. R., Filippelli, G., Föllmi, K., Shields, G., and Zanin, Y.: Variations in the global phosphorus cycle. *SEPM Spec. P.*, 66, 21–33, <https://doi.org/10.2110/pec.00.66.0021>, 2010.

Costa, K. M., Russell, J. M., Vogel, H., and Bijaksana, S.: Hydrological connectivity and mixing of Lake Towuti, Indonesia, in response to paleoclimatic changes over the last 60,000 years, *Palaeogeogr. Palaeocl.*, 417, 467–475, <https://doi.org/10.1016/j.palaeo.2014.10.009>, 2015.

Crosby, H. A., Roden, E. E., Johnson C. M., and Beard, B. L.: The mechanisms of iron isotope fractionation produced during dissimilatory Fe(III) reduction by *Shewanella putrefaciens* and *Geobacter sulfurreducens*, *Geobiology*, 5, 169–189, <https://doi.org/10.1111/j.1472-4669.2007.00103.x>, 2007.

Crowe, S. A., Pannalal, S. J., Fowle, D. A., Cioppa, M. T., Symons, D. T. A., Haffner, G. D., and Fryer, B. J.: Biogeochemical cycling in Fe-rich sediments from Lake Matano, Indonesia, *Int. Symp. Water-Rock Interact.*, 11, 1185–1189, 2004.

Crowe, S. A., Katsev, S., Hehanussa, P., Haffner, G. D., Sundby, B., Mucci, A., and Fowle, D. A.: The biogeochemistry of tropical lakes: A case study from Lake Matano, Indonesia, *Limnol. Oceanogr.*, 53, 319–331, <https://doi.org/10.4319/lo.2008.53.1.0319>, 2008.

Dauphas, N., John, S. G., and Rouxel, O.: Iron isotope systematics, *Rev. Mineral. Geochem.*, 82, 415–510, <https://doi.org/10.2138/rmg.2017.82.11>, 2017.

Dijkstra, N., Slomp, C. P., Behrends, T., and Expedition 347 Scientists: Vivianite is a key sink for phosphorus in sediments of the Landsort Deep, an intermittently anoxic deep basin in the Baltic Sea, *Chemic. Geol.*, 438, 58–72, <https://doi.org/10.1016/j.chemgeo.2016.05.025>, 2016.

Egger, M., Jilbert, T., Behrends, T., Rivard, C., and Slomp, C. P.: Vivianite is a major sink for phosphorus in methanogenic coastal surface sediments, *Geochim. Cosmochim. Ac.*, 169, 217–235, <https://doi.org/10.1016/j.gca.2015.09.012>, 2015.

Fagel, N., Alleman, L. Y., Granina, L., Hatert, F., Thamo-Bozso, E., Cloots, R., and Andre, L.: Vivianite formation and distribution in Lake Baikal sediments, *Glob. Planet. Change*, 46, 315–336, <https://doi.org/10.1016/j.gloplacha.2004.09.022>, 2005.

Ferris, F. G., Fyfe, W. S., and Beveridge, T. J.: Bacteria as nucleation sites for authigenic minerals in a metal-contaminated lake sediment, *Chem. Geol.*, 63, 252–232, <https://doi.org/10.1016/B978-0-444-88900-3.50035-7>, 1987.

Fredrickson, J. K., Zachara, J. M., Kennedy, D. W., Dong, H., Onstott, T. C., Hinman, N. W., and Li, S.: Biogenic iron mineralization accompanying the dissimilatory reduction of hydrous ferric oxide by a groundwater bacterium, *Geochim. Cosmochim. Ac.*, 62, 3239–3257, [https://doi.org/10.1016/S0016-7037\(98\)00243-9](https://doi.org/10.1016/S0016-7037(98)00243-9), 1998.

Friese, A., Kallmeyer, J., Kitte J. A., Montaño Martinez, I., Bijaksana, S., Wagner, D., the ICDP Lake Chalco Drilling Science Team, and the ICDP Towuti Drilling Science Team: A simple and inexpensive technique for assessing contamination during drilling operations, *Limnol. Oceanogr. Methods*, 15, 200–211, <https://doi.org/10.1002/lom3.10159>, 2017.

Friese, A., Kallmeyer, J., Glombitza, C., Vuillemin, A., Simister, R., Nomosatryo, S., Bauer, K., Heuer, V. B., Henny, C., Crowe, S. A., Ariztegui, D., Bijaksana, S., Vogel, H., Melles, M., Russell, J. M., and Wagner, D.: Methanogenesis predominates organic matter remineralization in a ferruginous, non-sulfidic sedimentary environment, *EGU General Assembly Conference Abstracts*, 20, 7446, 2018.

Gächter, R., Meyer, J. S., and Mares, A.: Contribution of bacteria to release and fixation of phosphorus in lake sediments, *Limnol. Oceanogr.*, 33, 1542–1558, https://doi.org/10.4319/lo.1988.33.6_part_2.1542, 1988.

Gächter, R., and Müller, B.: Why the phosphorus retention of lakes does not necessarily depend on the oxygen supply to their sediment surface, *Limnol. Oceanogr.*, 48, 929–933, <https://doi.org/10.4319/lo.2003.48.2.0929>, 2003.

Glasauer, S., Weidler, P. G., Langley, S., and Beveridge, T. J.: Controls on Fe reduction and mineral formation by a subsurface bacterium, *Geochim. Cosmochim. Ac.*, 67, 1277–1288, [https://doi.org/10.1016/S0016-7037\(02\)01199-7](https://doi.org/10.1016/S0016-7037(02)01199-7), 2003.

Golightly, J. P.: Progress in understanding the evolution of nickel laterites, in: *The Challenge of Finding New Mineral Resources - Global Metallogeny, Innovative Exploration, and New Discoveries*, Special Publication 15, Society of Economic Geologists, Denver, United-States, 451–485, 2010.

Golubev, S. V., Bénézeth, P., Schott, J., Dandurand, J. L., and Castillo, A.: Siderite dissolution kinetics in acidic aqueous solutions from 25 to 1000° C and 0 to 50 atm pCO₂, *Chem. Geol.*, 265, 13–19, <https://doi.org/10.1016/j.chemgeo.2008.12.031>, 2009.

Haffner, G. D., Hehanussa, P. E., and Hartoto, D.: The biology and physical processes of large lakes of Indonesia: Lakes Matano and Towuti, in: The Great Lakes of the World (GLOW): Food-Web, Health, and Integrity, edited by Munawar, M., and Hecky, R.E., Blackhuys, 183-194, 2001.

Halevy, I., Alesker, M., Schuster, E. M., Popovitz-Biro, R., and Feldman, Y.: A key role for green rust in the Precambrian oceans and the genesis of iron formations, *Nat. Geosci.*, 10, 135–139, <https://doi.org/10.1038/ngeo2878>, 2017.

Hansen, H. C. B., and Poulsen, I. F.: Interaction of synthetic sulphate "green rust" with phosphate and the crystallization of vivianite, *Clay. Clay Miner.*, 47, 312-318, doi: 10.1346/CCMN.1999.0470307, 1999.

Hanzel, D., Melsel, W., Hanzel, D., and Gütlich, P.: Mössbauer effect study of the oxidation of vivianite, *Solid State Commun.*, 76, 307-310, [https://doi.org/10.1016/0038-1098\(90\)90843-Z](https://doi.org/10.1016/0038-1098(90)90843-Z), 1990.

10 Harper, M., Howorth, R., and McLeod, M.: Late Holocene diatoms in Lake Poukawa: Effects of airfall tephra and changes in depth, *New Zeal. J. Mar. Fresh.*, 20, 107-118, <https://doi.org/10.1080/00288330.1986.9516135>, 1986.

Hasberg, A. K. M., Bijaksana, S., Held, P., Just, J., Melles, M., Morlock, M. A., Opitz, S., Russell, J. M., Vogel, H., and Wennrich, V.: Modern sedimentation processes in Lake Towuti, Indonesia, revealed by the composition of surface sediments, *Sedimentology*, 66, 675-698, <https://doi.org/10.1111/sed.12503>, 2019.

15 Henkel, S., Kasten, S., Poulton, S. W., and Staubwasser, M.: Determination of the stable iron isotopic composition of sequentially leached iron phases in marine sediments. *Chem. Geol.* 421, 93-102, <https://doi.org/10.1016/j.chemgeo.2015.12.003>, 2016.

Herschy, B., Chang, S. J., Blake, R., Lepland, A., Abbott-Lyon, H., Sampson, J., Atlas, Z., Kee, T. P., and Pasek, M. A.: Archean phosphorus liberation induced by iron redox geochemistry, *Nat. Commun.*, 9, 1346, <https://doi.org/10.1038/s41467-018-03835-3>, 2018.

20 Holland, H. D.: The oxygenation of the atmosphere and oceans, *Philos. T. Roy. Soc. B*, 361, 903-915, <https://doi.org/10.1098/rstb.2006.1838>, 2006.

Hupfer, M., and Lewandowski, J.: Oxygen controls the phosphorus release from lake sediments – a long-lasting paradigm in limnology, *Int. Rev. Hydrobiol.*, 93, 415–432, <https://doi.org/10.1002/iroh.200711054>, 2008.

25 Jenkins, S. R., and Moore, R. C.: A proposed modification to the classical method of calculating alkalinity in natural waters, *J. Am. Water Works Ass.* 69: 56-60, <https://doi.org/10.1002/j.1551-8833.1977.tb02544.x>, 1977.

Johnson, C. M., Roden, E. E., Welch, S. A., Beard, B. L.: Experimental constraints on Fe isotope fractionation during magnetite and Fe carbonate formation coupled to dissimilatory hydrous ferric oxide reduction, *Geochem. Cosmochim. Ac.*, 69, 963-993, <https://doi.org/10.1016/j.gca.2004.06.043>, 2005.

30 Johnson, C. M., Ludois, J. M., Beard, B. L., Beukes, N. J., and Heimann, A.: Iron formation carbonates: Paleoceanographic proxy or recorder of microbial diagenesis? *Geology*, 41, 1147-1150, <https://doi.org/10.1130/G34698.1>, 2013.

Johnson, C. A., Murayama, M., Küsel, K., Hochella, M. F. Jr.: Polycrystallinity of green rust minerals and their synthetic analogs: Implications for particle formation and reactivity in complex systems, *Am. Mineral.*, 100, 2091-2105, <https://doi.org/10.2138/am-2015-5287>, 2015.

Jones, C., Crowe, S. A., Sturm, A., Leslie, K. L., MacLean, L. C. W., Katsev, S., Henny, C., and Canfield, D. E.: Biogeochemistry of manganese in ferruginous Lake Matano, Indonesia: *Biogeosciences*, 8, 2977-2991, <https://doi.org/10.5194/bg-8-2977-2011>, 2011.

Jones, C., Nomosatryo, S., Crowe, S. A., Bjerrum, C. J., and Canfield, D. E.: Iron oxides, divalent cations, silica, and the early earth phosphorus crisis, *Geology*, 43, 135-138, <http://doi.org/10.1130/G36044.1>, 2015.

Katsev, S., Tsandev, I., L'Heureux, I., and Rancourt, D. G.: Factors controlling long-term phosphorus efflux from lake sediments: Exploratory reactive-transport modeling, *Chem. Geol.*, 234, 127-147, <https://doi.org/10.1016/j.chemgeo.2006.05.001>, 2006.

Katsev, S., Crowe, S. A., Mucci, A., Sundby, B., Nomosatryo, S., Haffner, G. D., and Fowle, D. A.: Mixing and its effects on biogeochemistry in the persistently stratified, deep, tropical Lake Matano, Indonesia, *Limnol. Oceanogr.*, 55, 763-776, <https://doi.org/10.4319/lo.2010.55.2.0763>, 2010.

Kipp, M. A., and Stüeken, E. E.: Biomass recycling and Earth's early phosphorus cycle, *Sci. Adv.*, 3, eaao4795, <https://doi.org/10.1126/sciadv.aao4795>, 2017.

Konhauser, K. O., LaLonde, S. V., Amskold, L., and Holland, H. D.: Was there really an Archean phosphate crisis?, *Science*, 315, 1234, <https://doi.org/10.1126/science.1136328>, 2007.

Lehmusluoto, P., Machbub, B., Terangna, N., Rumiputro, S., Achmad, F., Boer, L., Brahmana, S. S., Priadi, B., Setiadji, B., Sayuman, O., Margana, A.: National inventory of the major lakes and reservoirs in Indonesia. General limnology. Expedition Indodanau Technical Report. 1995.

Lemos, V. P., da Costa, M. L., Lemos, R. L., and de Faria, M. S. G.: Vivianite and siderite in lateritic iron crust: an example of bioreduction, *Quim. Nova*, 30, 36-40, <https://doi.org/10.1590/S0100-40422007000100008>, 2007.

Lenstra, W. K., Egger, M., van Helmond, N. A. G. M., Kritzberg, E., Conley, D. J., and Slomp, C. P.: Large variations in iron input to an oligotrophic Baltic Sea estuary: impact on sedimentary phosphorus burial, *Biogeosciences*, 15, 6979-6996, <https://doi.org/10.5194/bg-15-6979-2018>, 2018.

Manheim, F. T.: A hydraulic squeezer for obtaining interstitial water from consolidated and unconsolidated sediments, USGS Reference Paper, 550, 171-174, 1966.

Liu, K., Wu, L. L., Couture, R. M., Li, W. Q., and Van Cappellen, P.: Iron isotope fractionation in sediments of an oligotrophic freshwater lake, *Earth Planet. Sc. Lett.*, 423, 164-172, <https://doi.org/10.1016/j.epsl.2015.05.010>, 2015.

Maher, B. A., Alekseev, A., and Alekseeva, T.: Magnetic mineralogy of soils across the Russian Steppe: climatic dependence of pedogenic magnetite formation. *Palaeogeogr. Palaeocl.* 201, 321-341, doi: 10.1016/S0031-0182(03)00618-7, 2003.

Manning, P. G., Murphy, T. P., and Prepas, E. E.: Intensive formation of vivianite in the bottom sediments of mesotrophic Narrow Lake, Alberta, *Can. Mineral.*, 29, 77-85, 1991.

Michiels C.C., Darchambeau, F., Roland, F. A., Morana, C., Llirós, M., Garcia-Armisen, T., Thamdrup, B., Borges, A. V., Canfield, D. E., Servais, P., Descy, J.-P., and Crowe, S. A.: Iron-dependent nitrogen cycling in a ferruginous lake and the nutrient status of Proterozoic oceans, *Nat. Geosci.*, 10, 217-221, <https://doi.org/10.1038/NGO2886>, 2017.

Morlock, M. A., Vogel, H., Nigg, V., Ordoñez, L., Hasberg, A. K. M., Melles, M., Russell, J. M., Bijaksana, S., and the TDP 5 Science Team: Climatic and tectonic controls on source-to-sink processes in the tropical, ultramafic catchment of Lake Towuti, Indonesia, *J. Paleolimnol.*, 61, 279-295, <https://doi.org/10.1007/s10933-018-0059-3>, 2019.

Murphy, J., and Riley, J. P.: A modified single solution method for the determination of phosphate in natural waters, *Anal. Chim. Acta*, 27, 31-36, [https://doi.org/10.1016/S0003-2670\(00\)88444-5](https://doi.org/10.1016/S0003-2670(00)88444-5), 1962.

Nomosatryo, S., Henny, C., Jones, C. A., Michiels, C., and Crowe, S. A.: Karakteristik dan klasifikasi trofik di Danau 10 Matano dan Danau Towuti Sulawesi selatan, Perkembangan Limnologi dalam Mendukung Pembangunan Berkelanjutan di Indonesia: Tantangan dan Harapan, Prosiding Pertemuan Ilmiah Tahunan MLI I, 493-507, 2013.

Nanzyo, M., Takahashi, T., Sato, A., Shoji, S., and Yamada, I: Dilute acid-soluble phosphorus in fresh air-borne tephras and fixation with an increase in active aluminium and iron, *Soil Sci. Plant. Nutr.*, 43, 839-848, <https://doi.org/10.1080/00380768.1997.10414650>, 1997.

O'Loughlin, E. J., Boyanov, M. I., Flynn, T. M., Gorski, C. A., Hofmann, S. M., McCormick, M. L., Scherer, M. M., and Kemner, K. M.: Effects of bound phosphate on the bioreduction of lepidocrocite (γ -FeOOH) and maghemite (γ -Fe₂O₃) and formation of secondary minerals, *Environ. Sci. Technol.*, 47, 9157-9166, <https://doi.org/10.1021/es400627j>, 2013.

Ordoñez, L., Vogel, H., Sebag, D., Ariztegui, D., Adatte, T., Russell, J.M., Kallmeyer, J., Vuillemin, A., Friese, A., Crowe, S.A., Bauer, K.W., Simister, R., Nomosatryo, S., Henny, C., and Bijaksana, S.: Empowering conventional Rock-Eval 20 pyrolysis for organic matter characterization of the siderite-rich sediments of Lake Towuti (Indonesia) using End-Member Analysis. *Org. Geochem.*, 134, 32-44, <https://doi.org/10.1016/j.orggeochem.201905.002>, 2019.

Parkhurst, D. L., and Appelo, C. A. J. (Eds.): *Description of input and examples for PHREEQC version 3 - A computer program for speciation, batch-reaction, one-dimensional transport, and inverse geochemical calculations*, book 6, chapter A43: U.S. Geological Survey Techniques and Methods, Denver, USA, 2013.

Percak-Dennett, E. M., Loizeau, J. L., Beard, B. L., Johnson, C. M., and Roden, E. E.: Iron isotope geochemistry of biogenic 25 magnetite-bearing sediments from the Bay of Vidy, Lake Geneva, *Chem. Geol.*, 360, 32-40, <https://doi.org/10.1016/j.chemgeo.2013.10.008>, 2013.

Postma, D.: Formation of siderite and vivianite and the pore water composition of a recent bog sediment in Denmark. *Chem. Geol.*, 31, 225-244, [https://doi.org/10.1016/0009-2541\(80\)90088-1](https://doi.org/10.1016/0009-2541(80)90088-1), 1981.

Poulton, S. W., and Canfield, D. E.: Development of a sequential extraction procedure for iron: implications for iron 30 partitioning in continentally derived particulates. *Chem. Geol.*, 214, 209-221, <https://doi.org/10.1016/j.chemgeo.2004.09.003>, 2005.

Prieto, F. J. M., and Millero, F. J.: The values of pK1 + pK2 for the dissociation of carbonic acid in seawater, *Geochim. Cosmochim. Ac.*, 66, 2529–2540, [https://doi.org/10.1016/S0016-7037\(02\)00855-4](https://doi.org/10.1016/S0016-7037(02)00855-4), 2002.

Recasens, C., Ariztegui, D., Maidana, N. I., Zolitschka, B., and the PASADO Science Team: Diatoms as indicators of hydrological and climatic changes in Laguna Potrok Aike (Patagonia) since the Late Pleistocene, *Palaeogeogr. Palaeocl.* 417, 309–319, <https://doi.org/10.1016/j.palaeo.2014.09.021>.

Reed, D. C., Slomp, C. P., and Gustafsson, B. G.: Sedimentary phosphorus dynamics and the evolution of bottom-water hypoxia: A coupled benthic-pelagic model of a coastal system, *Limnol. Oceanogr.*, 56, 1075–1092, <https://doi.org/10.4319/lo.2011.56.3.1075>, 2011.

Reed, D. C., Gustafsson, B. G., and Slomp, C. P.: Shelf-to-basin iron shuttling enhances vivianite formation in deep Baltic Sea sediments, *Earth Planet. Sc. Lett.*, 434, 241–251, <https://doi.org/10.1016/j.epsl.2015.11.033>, 2016.

Refaat, P., Reffass, M., Landoulsi, J., Sabot, R., and Jeannin, M.: Role of phosphate species during the formation and transformation of the Fe(II–III) hydroxycarbonate green rust, *Colloid. Surface A.*, 299, 29–37, doi: [10.1016/j.colsurfa.2006.11.013](https://doi.org/10.1016/j.colsurfa.2006.11.013), 2007.

Roden, E. E., and Edmonds, J. W.: Phosphate mobilization in iron-rich anaerobic sediments: microbial Fe(III) oxide reduction versus iron-sulfide formation, *Arch. Hydrobiol.*, 139, 347–378, <https://doi.org/0003-9136/97/0139-0347>, 1997.

Rothe, M., Frederick, T., Eder, M., Kleeberg, A., and Hupfer, M.: Evidence for vivianite formation and its contribution to long-term phosphorus retention in a recent lake sediment: a novel analytical approach, *Biogeosciences*, 11, 5169–5180, <https://doi.org/10.5194/bg-11-5169-2014>, 2014.

Rothe, M., Kleeberg, A., Grüneberg, B., Friese, K., Pérez- Mayo, M., and Hupfer, M.: Sedimentary sulphur:iron ratio indicates vivianite occurrence: A study from two contrasting freshwater systems, *PLoS ONE*, 10, e0143737, <https://doi.org/10.1371/journal.pone.0143737>, 2015.

Rothe, M., Kleeberg, A., and Hupfer, M.: The occurrence, identification and environmental relevance of vivianite in waterlogged soils and aquatic sediments, *Earth Sci. Rev.*, 158, 51–64, <https://doi.org/10.1016/j.earscirev.2016.04.008>, 2016.

Russell, J. M., Vogel, H., Konecky, B. L., Bijaksana, S., Huang, Y., Melles, M., Watrus, N., Costa, K., and King, J. W.: Glacial forcing of central Indonesian hydroclimate since 60,000 y B.P., *P. Natl. Acad. Sci.*, 111, 5100–5105, <https://doi.org/10.1073/pnas.1402373111>, 2014.

Russell, J. M., Bijaksana, S., Vogel, H., Melles, M., Kallmeyer, J., Ariztegui, D., Crowe, S., Fajar, S., Hafidz, A., Haffner, D., Hasberg, A., Ivory, S., Kelly, C., King, J., Kirana, K., Morlock, M., Noren, A., O'Grady, R., Ordonez, L., Stevenson, J., von Rintelen, T., Vuillemin, A., Watkinson, I., Watrus, N., Wicaksono, S., Wonik, T., Bauer, K., Deino, A., Friese, A., Henny, C., Imran, Marwoto, R., Ngkoimani, L. O., Nomosatryo, S., Safiuddin, L. O., Simister, R., and Tamuntuan, G.: The Towuti Drilling Project: Paleoenvironments, biological evolution, and geomicrobiology of a tropical Pacific lake, *Sci. Dri.*, 21, 29–40, <https://doi.org/10.5194/sd-21-29-2016>, 2016.

Sánchez-Román, M., Puente-Sánchez, F., Parro, V., and Amils, R.: Nucleation of Fe-rich phosphate and carbonate on microbial cells and exopolymeric substances. *Front. Microbiol.*, 6, 1024, <https://doi.org/10.3389/fmicb.2015.01024>, 2015.

Sapota, T., Aldahan, A., and Al-Aasm, I. S.: Sedimentary facies and climate control of formation of vivianite and siderite microconcretions in sediments of Lake Baikal, Siberia, *J. Paleolimnol.*, 36, 245–257, <https://doi.org/10.1007/s10933-006-9005-x>, 2006.

Schoenberg, R., and von Blanckenburg, F.: An assessment of the accuracy of stable Fe isotope ratio measurements on samples with organic and inorganic matrices by high-resolution multicollector ICP-MS, *Int. J. Mass Spectrom.*, 242, 257-272, <https://doi.org/10.1016/j.ijms.2004.11.025>, 2005.

Scholz, F., Severmann, S., McManus, J., Noffke, A., Lomnitz, U., and Hensen, C.: On the isotope composition of reactive iron in marine sediments: Redox shuttle versus early diagenesis. *Chem. Geol.*, 389, 48-59, <https://doi.org/10.1016/j.chemgeo.2014.09.009>, 2014.

10 Schütt, B.: Reconstruction of Holocene paleoenvironments in the endorheic basin of Laguna de Gallocanta, Central Spain by investigation of mineralogical and geochemical characters from lacustrine sediments *J. Paleolimnol.* 20, 217-234, <https://doi.org/10.1023/A:1007924000636>, 1998.

Severmann, S., Johnson, C. M., Beard, B. L., and McManus, J.: The effect of early diagenesis on the Fe isotope compositions of porewaters and authigenic minerals in continental margin sediments, *Geochim. Cosmochim. Ac.*, 70, 2006-2022, <https://doi.org/10.1016/j.gca.2006.01.007>, 2006.

Seward, R. W. (Ed.): NBS Standard Reference Material Catalog NBS, Special Publication 260, National Bureau of Standards, Gaithersburg, USA, 1986-1987.

Shaffer, G.: Phosphate pumps and shuttles in the Black Sea. *Nature* 321, 515-517. <https://doi.org/10.1038/321515a0>.

Sheppard, R. Y., Milliken, R. E., Russell, J. M., Darby Dyar, M., Sklute, E. C., Vogel, H., Melles, M., Bijaksana, S., 20 Morlock, M. A., and Hasberg, A. K. M.: Characterization of iron in Lake Towuti sediment. *Chem. Geol.* 512, 11-30. <https://doi.org/10.1016/j.chemgeo.2019.02.029>, 2019.

Singh, B., Sherman, D. M., Gilkes, R. J., Wells, M., and Mosselmans, J. F. W.: Structural chemistry of Fe, Mn, and Ni in synthetic hematites as determined by extended X-ray absorption fine structure spectroscopy, *Clay Clay Miner.*, 48, 521-527, <https://doi.org/10.1346/CCMN.2000.0480504>, 2000.

25 Skulan, J. L., Beard, B. L., and Johnson, C. M.: Kinetic and equilibrium Fe isotope fractionation between aqueous Fe(III) and hematite. *Geochim. Cosmochim. Ac.*, 66, 2995-3015, [https://doi.org/10.1016/S0016-7037\(02\)00902-X](https://doi.org/10.1016/S0016-7037(02)00902-X), 2002.

Song, L. T., Liu, C., Wang, Z., Zhu, X., Teng, Y., Wang, J., Tang, S., Li, J., and Liang, L.: Iron isotope compositions of natural river and lake samples in the karst area, Guizhou Province, Southwest China, *Acta Geol. Sin.-Engl.*, 85, 712-722, <https://doi.org/10.1111/j.1755-6724.2011.00464.x>, 2011.

30 Stamatakis, M. G., and Koukouzas, N. K.: The occurrence of phosphate minerals in lacustrine clayey diatomite deposits, Thessaly, Central Greece, *Sediment. Geol.*, 139, 33-47, [https://doi.org/10.1016/S0037-0738\(00\)00154-8](https://doi.org/10.1016/S0037-0738(00)00154-8), 2001.

Stookey, L. L.: Ferrozine - A new spectrophotometric reagent for iron, *Anal. Chem.*, 42, 779-781, <https://doi.org/10.1021/ac60289a016>, 1970.

Staubwasser, M., von Blanckenburg, F., and Schoenberg, R.: Iron isotopes in the early marine diagenetic iron cycle, *Geology*, 34, 629-632, <https://doi.org/10.1130/622647.1>, 2006.

Tamuntuan, G., Bijaksana, S., King, J., Russell, J., Fauzi, U., and Maryunani, K.: Variation of magnetic properties in sediments from Lake Towuti, Indoensia, and its paleoclimatic significance, *Palaeogeogr. Palaeoclimatol. Palaeoecol.*, 420, 163–172, <https://doi.org/10.1016/j.palaeo.2014.12.008>, 2015.

Tangalos, G. E., Beard, B. L., and Johnson, C. M.: Microbial production of isotopically light iron(II) in a modern chemically precipitated sediment and implications for isotopic variations in ancient rocks, *Geobiology*, 8, 197-208, <https://doi.org/10.1111/j.1472-4669.2010.00237.x>, 2010.

Teutsch, N., Schmid, M., Müller, B., Halliday, A. N., Bürgmann, H., and Wehrli, B.: Large iron isotope fractionation at the oxic-anoxic boundary in Lake Nyos. *Earth Planet. Sc. Lett.*, 285, 52-60, <https://doi.org/10.1016/j.epsl.2009.05.044>, 2009.

Trolard, F., Bourrié, G., Abdelmoula, M., Refait, P., and Feder, F.: Fougèrite, a new mineral of the pyroaurite-iowaite group: Description and crystal structure, *Clay Clay Miner.*, 55, 323-334, <https://doi.org/10.1346/CCMN.2007.0550308>, 2007.

Van der Grinten, E., Janssen, M., Simis, S. G. H., Barranguet, C., and Admiraal, W.: Phosphate regime structures species composition in cultured phototrophic biofilms, *Freshwater Biol.*, 49, 369-381, <https://doi.org/10.1111/j.1365-2427.01189.x>, 2004.

Vogel, H., Russell, J. M., Cahyarini, S. Y., Bijaksana, S., Watrus, N., Rethemeyer, J., and Melles, M.: Depositional modes and lake-level variability at Lake Towuti, Indonesia, during the past ~29 kyr BP, *J. Paleolimnol.*, 54, 359-377, [https://doi.org/10.1016/S0883-2927\(99\)00097-9](https://doi.org/10.1016/S0883-2927(99)00097-9), 2015.

Vodyanitskii, Y. N., and Shoba, S. A.: Ephemeral Fe(II)/Fe(III) layered double hydroxides in hydromorphic soils: A review, *Eurasian Soil Sci.*, 48, 240-249, doi: 10.1134/S10642293150, 2015.

Viollier, E., Inglett, P. W., Hunter, K., Roychoudhury, A. N., and Van Cappellen P.: The ferrozine method revisited: Fe(II)/Fe(III) determination in natural waters. *Appl. Geochem.*, 15, 785-790, [https://doi.org/10.1016/S0883-2927\(99\)00097-9](https://doi.org/10.1016/S0883-2927(99)00097-9), 2000.

von Blanckenburg, F., Marnberti, M., Schoenberg, R., Kamber, B. S., and Webb, G. E.: The iron isotope composition of microbial carbonate, *Chem. Geol.*, 249, 113-128, <https://doi.org/10.1016/j.chemgeo.2007.12.001>, 2008.

von Blanckenburg, F., Wittmann, H., and Schuessler, J. A.: HELGES: Helmholtz Laboratory for the Geochemistry of the Earth Surface. *Journal of Large-Scale Research Facilities*, 2, <https://doi.org/10.17815/jlsrf-2-141>, 2016.

Vuillemin, A., Ariztegui, D., Coninck, A., Lücke, A., Mayr, C., Schubert, C., and the PASADO Scientific Team: Origin and significance of diagenetic concretions in sediments of Laguna Potrok Aike, southern Argentina, *J. Paleolimnol.*, 50, 275–291, <https://doi.org/10.1007/s10933-013-9723-9>, 2013.

Vuillemin, A., Ariztegui, D., Lücke, A., Mayr, C., and the PASADO Science Team: Paleoenvironmental conditions define current sustainability of microbial populations in Laguna Potrok Aike, Argentina, *Aquat. Sci.*, 76, 101-114, <https://doi.org/10.1007/s00027-013-0317-4>, 2014.

Vuillemin, A., Friese, A., Alawi, M., Henny, C., Nomosatryo, S., Wagner, D., Crowe, S. A., and Kallmeyer, J.: Geomicrobiological features of ferruginous sediments from Lake Towuti, Indonesia, *Front. Microbiol.*, 7, e1007, <https://doi.org/10.3389/fmicb.2016.01007>, 2016.

Vuillemin, A., Horn, F., Alawi, M., Henny, C., Wagner, D., Crowe, S. A., and Kallmeyer, J.: Preservation and significance of extracellular DNA in ferruginous sediments from Lake Towuti, Indonesia, *Front. Microbiol.*, 8, e1440, <https://doi.org/10.3389/fmicb.2017.01440>, 2017.

Vuillemin, A., Horn, F., Friese, A., Winkel, M., Alawi, M., Wagner, D., Henny, C., Orsi, W. D., Crowe, S. A., and Kallmeyer, J.: Metabolical potential of microbial communities from ferruginous sediments. *Environ. Microbiol.*, 20, 4297-4313, <https://doi.org/10.1111/1462-2920.1443>, 2018.

10 Vuillemin, A., Wirth, R., Kemnitz, H., Schleicher, A.M., Friese, A., Bauer, K.W., Simister, R., Nomosatryo, S., Ordoñez, L., Ariztegui, D., Henny, C., Crowe, S.A., Benning, L.G., Kallmeyer, J., Russell, J.M., Bijaksana, S., Vogel, H., and the Towuti Drilling Project Science Team: Formation of diagenetic siderite in modern ferruginous sediments. *Geology* 47, 540-544, <https://doi.org/10.1130/G46100.1>, 2019a.

Vuillemin, A., Friese, A., Lücke, A., Bauer, K.W., Nomosatryo, S., Simister, R., Ordoñez, L.G., Ariztegui, D., Russell, J.M., 15 Bijaksana, S., Vogel, H., Crowe, S.A., Kallmeyer, J., and the Towuti Drilling Project Science Team: Pore water geochemistry and bulk sediment measurements of downcore profiles from site TDP-1A of the ICDP Towuti Drilling Project, Lake Towuti, Indonesia. Dataset #908080, doi: 10.1594/PANGAEA.908080, 2019b.

Wilson, T. A., Amirbahman, A., Norton, S. A., and Voytek, M. A.: A record of phosphorus dynamics in oligotrophic lake sediment, *J. Paleolimnol.*, 44, 279-294, <https://doi.org/10.1007/s10933-009-9403-y>, 2010.

20 Wirth, R.: Focused Ion Beam (FIB) combined with SEM and TEM: Advanced analytical tools for studies of chemical composition, microstructure and crystal structure in geomaterials on a nanometre scale, *Chem. Geol.*, 261, 217-229, <https://doi.org/10.1016/j.chemgeo.2008.05.019>, 2009.

Wu, L. L., Beard, B. L., Roden, E. E., and Johnson, C. M.: Stable iron isotope fractionation between aqueous Fe(II) and hydrous ferric oxide, *Environ. Sci. Technol.* 45, 1847-1852, <https://doi.org/10.1021/es103171x>, 2011.

25 Zachara, J. M., Fredrickson, J. K., Li, S. M., Kennedy, D. W., Smith, S. C., and Gassman, P. L.: Bacterial reduction of crystalline Fe³⁺ oxides in single phase suspensions and subsurface materials, *Am. Miner.*, 83, 1426-1443, <https://doi.org/10.2138/am-1998-1105>, 1998.

Zegeye, A., Bonneville, S., Benning, L. G., Sturm, A., Fowle, D. A., Jones, C., Canfield, D. E., Ruby, C., MacLean, L. C., Nomosatryo, S., Crowe, S. A., and Poulton, S. W.: Green rust formation controls nutrient availability in a ferruginous water column, *Geology*, 40, 599-602, <https://doi.org/10.1130/G32959.1>, 2012.

Zhang, Y., and Prepas, E. E.: Regulation of the dominance of planktonic diatoms and cyanobacteria in four eutrophic hardwater lakes by nutrients, water column stability, and temperature, *Can. J. Fish. Aquat. Sci.*, 53, 621-633, <https://doi.org/10.1139/f95-205>, 1996.

Figures

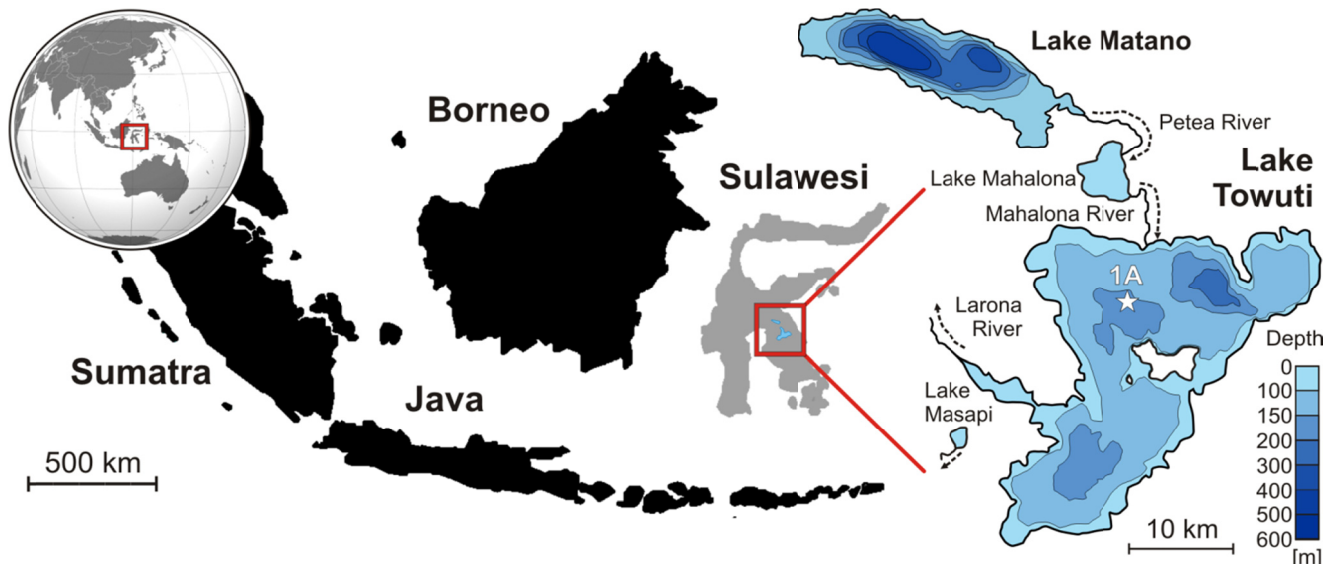


Figure 1: Location of the Malili Lake System and bathymetric map of Lake Matano and Towuti. (Left) World map displaying the location of Sulawesi Island (red square) with close-up on the Indonesia archipelago and location of the Malili Lake System (red square). (Right) Bathymetric map of Lake Matano and Lake Towuti with position of the ICDP drilling site TDP-1A from which hydraulic piston cores were retrieved and sampled for this study.

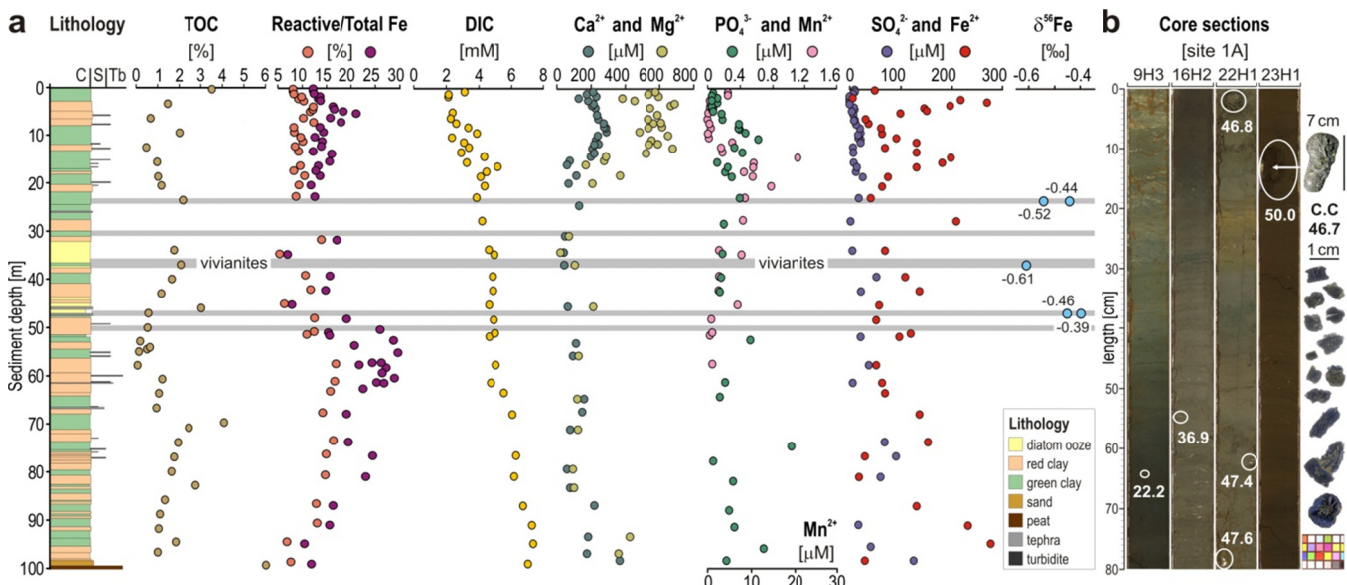


Figure 2: Stratigraphy of composite site TDP-1, multiple profiles established on sediment core subsamples, and core section images. (a) Stratigraphy of composite site TDP-1 (after Russell et al., 2016) and corresponding grain sizes (C: clay; S: silt; Tb: turbidite); total organic carbon (TOC), reactive and total iron [weight %] in bulk sediment; dissolved inorganic carbon (DIC) [mM], calcium, magnesium, phosphate, manganese, sulfate and ferrous iron concentrations [μM] measured in pore water; and δ⁵⁶Fe isotopic compositions of vivianite crystals. (b) Images of core sections from which vivianite crystals were hand-picked. Crystals on the far right were extracted from core catchers.

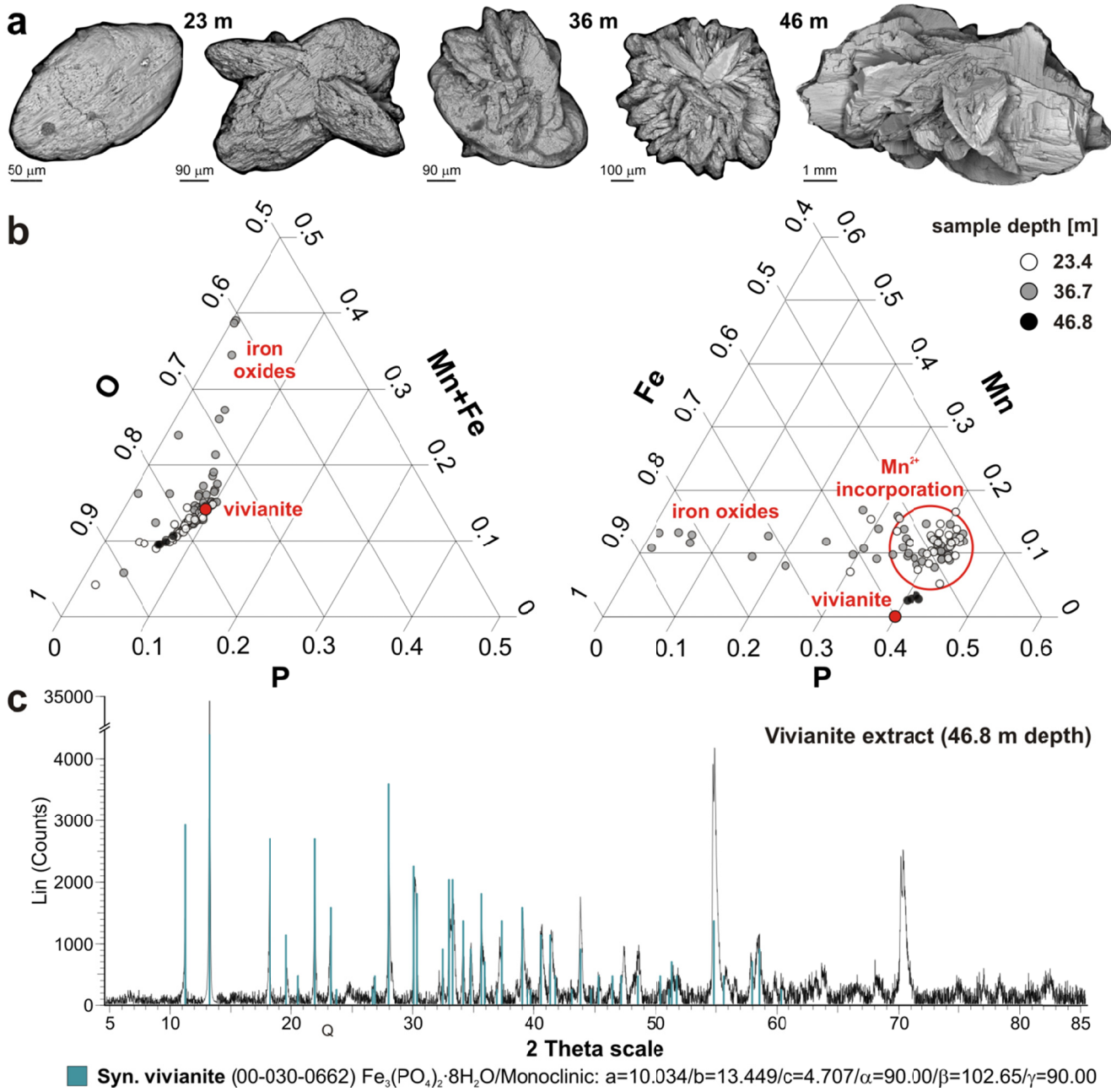


Figure 3: SEM images of vivianite crystals, ternary diagrams of EDX punctual analyses and XRD spectrum. (a) SEM images show that vivianite crystals grow from a tabular habit to rosette. (b) EDX elemental analyses (i.e. O, P, Fe, Mn) of vivianite crystals standardized to 100 % for each ternary diagram. Results indicate incorporation of manganese in the vivianites with the presence of detrital iron oxides. Deepest samples plot closer to stoichiometric vivianite (red dot). (c) XRD spectrum of pure vivianite extract from 46.8 m depth with reference peaks of synthetic vivianite (blue bars).

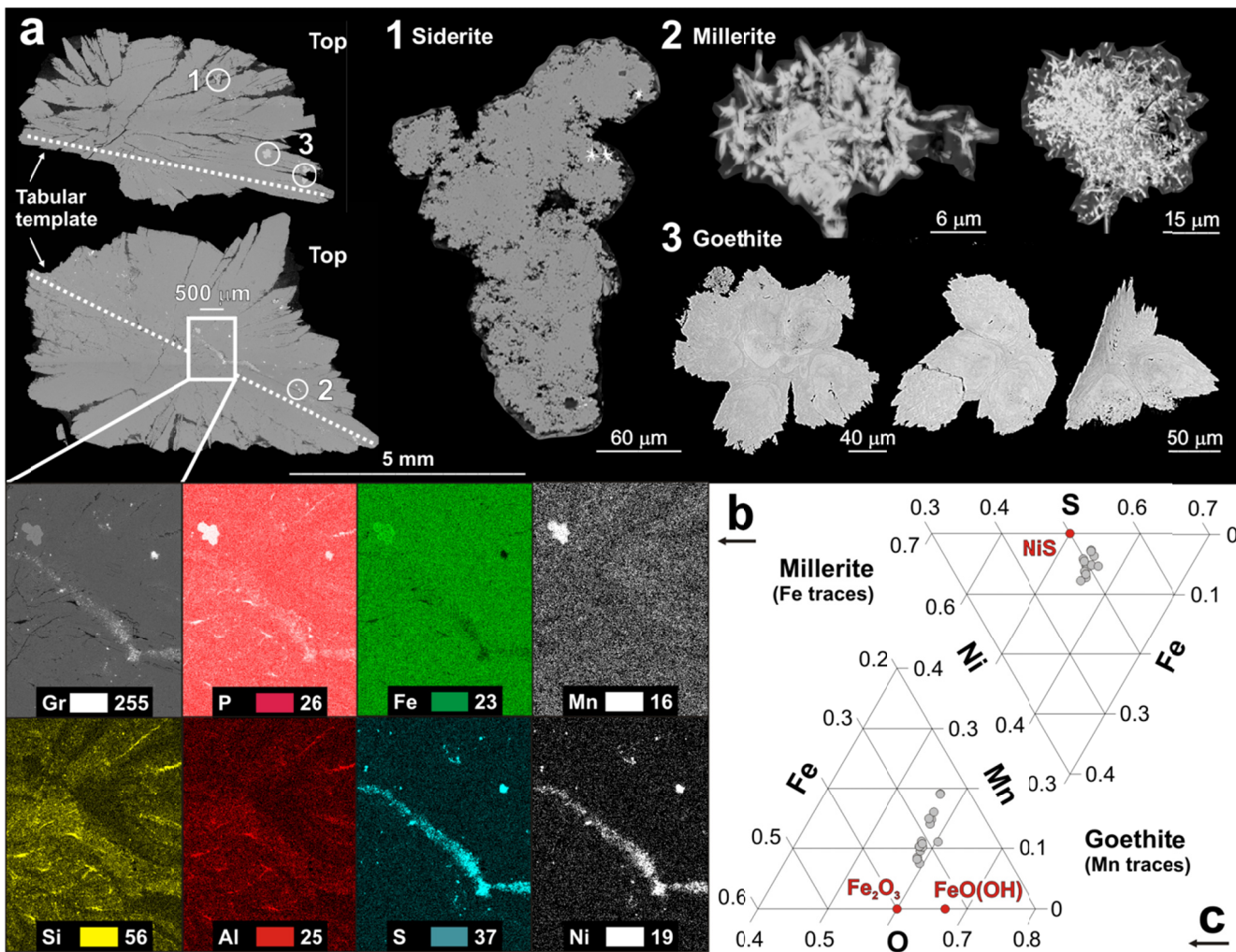


Figure 4: SEM images of vivianite crystal in axial section, and close-ups to mineral inclusions with EDX mapping and punctual analyses. (a) SEM images of an axial section of a vivianite crystal from 46.8 m depth, with inclusions of siderite (1), millerite (2) and goethite (3). **(b)** EDX elemental mapping of the framed area with relative intensity images for grey levels (Gr), phosphorus (P), iron (Fe), manganese (Mn), silicium (Si), aluminium (Al), sulfur (S) and nickel (Ni). **(c)** Ternary diagrams displaying the elemental composition of millerite and goethite as measured by punctual EDX analyses. Millerite and goethite crystals contain traces of iron and manganese, respectively.

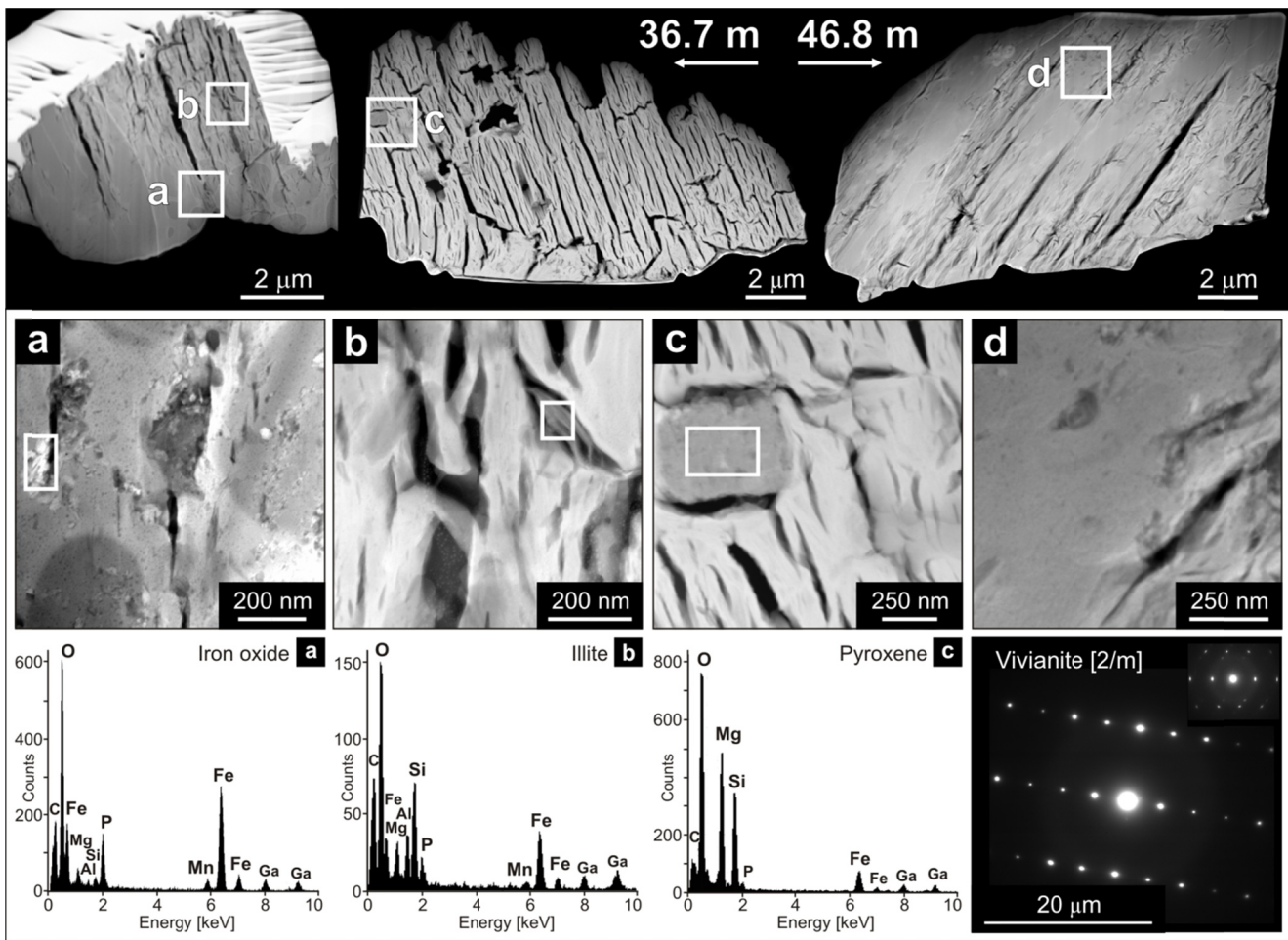


Figure 5: TEM images of vivianite crystal chunks, and close-ups to detrital inclusions with their EDX analyses and vivianite electron diffraction patterns. (Top) TEM images (distance: 330 mm) of vivianite crystal chunks from 36.7 and 46.8 m depth, showing that the crystal structure is denser in the deeper sample. (Middle) Close-ups of framed areas illustrate the presence of detrital inclusions within vivianite crystals, namely iron oxide (a), illite (b) and pyroxene (c). Image d demonstrates the denser structure of the vivianite crystal from 46.8 m depth. (Bottom) EDX spectra for iron oxide (a), illite (b) and pyroxene (c); and high-resolution electron diffraction pattern of the vivianites from 46.8 and 36.7 (insert) m depth providing evidence for an organized and less-organized monoclinic lattice.

Table

Table 1: Modeled saturation indices based on pH, alkalinity, pore water concentrations of major ions and borehole temperatures.
Siderite appears to be oversaturated throughout the sedimentary sequence, whereas vivianite remains close to, but slightly below saturation with sediment depth.

5

5 m depth	Saturation	10 m depth	Saturation
talc/serpentine	1.43	siderite	1.00
siderite	1.29	quartz	0.71
quartz	0.71	vivianite	-0.04
vivianite	-0.45	talc/serpentine	-0.31
calcite	-0.68	calcite	-0.83
dolomite	-0.77	aragonite	-0.97
aragonite	-0.82	dolomite	-1.27